PROJECT CELESCOPE

An Astrophysical Reconnaissance Satellite

Introduction

The Smithsonian Astrophysical Observatory has long been interested in artificial satellites. Since 1955, one of our primary missions has been the precision optical tracking of such satellites. By these passive observing techniques we have gained valuable information concerning upper atmospheric densities and the shape and structure of the earth.

Not only these satellites but also many recent rockets and balloons have contained active experimental apparatus for conducting observational programs above the atmosphere. Astronomers have three major reasons for making such observations. First, they want to overcome the problem of atmospheric absorption of electromagnetic radiation. The first solar spectrograms extending to wavelengths shorter than 2900 A were obtained from V-2 rockets flown in 1946. Another example is the John Hopkins balloon observations in 1959, during which Dr. Strong detected water-vapor bands in the infrared spectrum of Venus. The second reason is to increase angular resolution. Princeton's Project Stratoscope balloon program enabled Dr. Martin Schwarzschild in 1958 to photograph the solar granulation at improved resolution. The third reason is to decrease background illumination. There is as yet no example of extraterrestrial observations for this purpose.

On 4 and 25 February 1958, the scientific staffs of Harvard College Observatory and the Smithsonian Astrophysical Observatory met to discuss the most urgently needed astrophysical observations above the atmosphere. We concluded that the first should be ultraviolet studies, since infrared and high-resolution studies could at present be better done from balloons. We planned on using imaging techniques to allow us to study a maximum number of objects during the early phases of the program. Television offered advantages over other methods because it would enable us to control and change the program as the data were gathered.

In September of 1958, the Smithsonian Astrophysical Observatory presented to the National Aeronautics and Space Administration a research proposal for these ultraviolet television studies. From this proposal has grown Project Celescope, named for its pioneering use of a truly celestial telescope. The project is now a division of the Smithsonian Astrophysical Observatory and operates under NASA Grant No. NsG-51-60 and extensions. The NASA project that includes Celescope is the Orbiting Astronomical Observatories program (OAO), also termed the S-18 series. Other participating agencies are the University of Wisconsin, NASA's Goddard Space Flight Center, and Princeton University. The OAO program is more fully described by Ziemer (1961). The first OAO satellite, to be launched in 1963, will contain both the Celescope and the University of Wisconsin's experiment.

I. Astrophysical Background

Short-wave electromagnetic radiation reacts strongly with matter. At wavelengths longer than 3200 A, the effects of the earth's atmosphere can be rather well eliminated from observational data by proper reduction procedure. Below 2800 A, no appreciable amount of radiation can penetrate the atmosphere to balloon altitudes (approximately 30 km) or lower. Altitudes of at least 100 km are necessary for making reasonably good observations between 1000 and 3000 A.

No optical materials are transparent to wavelengths shorter than 1050 A. Since transparent materials are necessary in our television camera tubes, this sets our short-wavelength limit.

1. Absorption by the Earth's Atmosphere

Tousey (1961) gives a chart showing the depth of penetration of incident ultraviolet radiation into the atmosphere. With the exception of a small, dusky "window" near 2100 A, the level to which 37 percent of the incident radiation penetrates is above 300 km for all wavelengths shorter than 3000 A. Between 2000 and 3000 A, the absorption is caused primarily by ozone (O_3). Although the maximum ozone density occurs near 20 km (Vigroux, 1960), appreciable amounts extending above 30 km effectively block the radiation between 2200 and 2800 A.

Between 1000 and 2000 A, the absorption is produced primarily by molecular oxygen (O_2). Throughout most of this region, 37 percent of the incident radiation penetrates to a level near 100 km. The vertical distribution of molecular oxygen is discussed by Kamiyama (1959).

2. Stellar Atmospheres

Of the many problems to be attacked by the Celescope, only for the atmospheres of main-sequence early-type stars do we now have a reasonably clear picture of what to expect. One of Celescope's goals is the measurement of the brightnesses of about 100,000 such stars in three spectral bands between 1000 and 3000 A.

The datum of interest is the shape of the spectral-energy distribution curves of the different types of stars. As was the case with the great sky surveys of the past--e.g., the Henry Draper Catalog and the Palomar Sky Atlas--we plan to acquire our data by a survey of the entire available portion of the celestial sphere, and thus increase our chances of making important unexpected discoveries. We are planning our instrumentation and observational program so as to balance the payload limitations of the Celescope with these scientific objectives.

Celescope's instrumental sensitivity is such that only a few thousand stars would be bright enough to be measured when their light is spread out into spectra. Since we have room for four telescopes in Celescope's portion of the satellite, we have decided to install one slitless spectroscope and three broad-band mapping telescopes. The latter instruments will give us three points each in the ultraviolet spectral energy curves of about 100,000 stars, while the spectroscope gives us about 100 points each in the curves of about 5,000 stars.

The observational foundation for astrophysics is spectroscopy. Under close scrutiny, no two stellar spectra are identical. However, the great majority can be placed in a one-dimensional sequence based primarily on temperature. The coolest are the M stars, at about 3000° K. The K stars are at about 4200° K. (Both are also referred to as late-type stars, a relic of an obsolete theory of stellar evolution.) The G and F stars, intermediate types, are at about 6000° K. Early types are the A stars, at about 8000° K; the B stars, at about 15,000° K; and the O stars, at

about 40,000° K. Each of these seven types is divided numerically, with the "0" (zero) subdivision being hottest and 10 the coolest. Thus, a BO star at 32,800° K is nearly as hot as an O9 star at 37,450° K. The earliest O stars are classified as O5, and the latest M stars as M8. The sun is spectral type G1.5, at 5785° K.

To this one-dimensional temperature sequence may be added a second, less conspicuous, dimension involving atmospheric density. The giants and supergiants are less dense than the main-sequence (dwarf) stars, and therefore have sharper lines in their spectra. The giants and supergiants are much larger and more luminous than their main-sequence counterparts.

A third dimension in this scheme involves differences in chemical composition. Stars of types R, N, and S are cool stars of less usual chemical composition than the M stars. For the hotter stars, at least in the presently accessible region of the spectrum, these differences are not so obvious.

Many stars having somewhat peculiar spectra can still be fitted into the above scheme. Others, including the Wolf-Rayet stars, cannot. The Wolf-Rayet stars are apparently quite hot, exceeding 15,000° K, perhaps by a rather large factor. Their spectra consist primarily of emission lines and bands.

Figure 1 compares the computed spectral distributions of various stars with those of black bodies having the same total energy outputs--that is, with the same effective temperatures, $T_{eff} = (E_{out}/4\pi r^2 \sigma)^{1/4}$. Here, E_{out} is the energy output of a star of radius r; and σ is the Stefan-Boltzmann constant, 5.669×10^{-5} erg cm^{-2} sec^{-1} (° K)$^{-4}$. The theories used in the computation of the model atmospheres upon which figure 1 is based were developed primarily in the years 1950-1958. The newest theories, not yet fully evaluated, indicate that the curves shown in the figure may seriously overestimate the ultraviolet fluxes and the effective temperatures of the O and B stars (see Carrier and Avrett (1961), and Stone and Gaustad (1961)). The newest observations (Stecher and Milligan, 1961) also indicate that the ultraviolet fluxes of the O and B stars are lower than anticipated, perhaps by a factor of 30 at 1500 A.

The limiting sensitivity of the Celescope will be about 0.02 photon per square centimeter per Angstrom per second incident upon the optical system. As we can see from figure 1, the brightest star in each spectral class AO and earlier lies well above threshold, and we can expect to observe a large number of them with the Celescope. However, especially for the shorter wavelengths, even the brightest star of solar type (G1.5) and later lie rather near our threshold. Figure 2 indicates the number of stars of various spectral types that we expect to observe. The visual region is included for reference. As we shorten the effective wavelength of our photometric system, we get a smaller and smaller proportion of the later type stars.

This problem of the ultraviolet flux from hot stars is of great importance to theoretical astrophysics. One goal of Celescope is to give it an observational foundation, and to chart the path for observing programs and instrumentation for future, more specialized satellites that are being planned.

3. Interstellar Absorption

Although Sir William Herschel made extensive studies of the irregularities in apparent stellar distribution caused by interstellar dust, it was more than a century later that this irregular distribution was correctly ascribed to interstellar absorption. And although Hartmann (1904) correctly ascribed certain narrow absorption lines in stellar spectra to interstellar gas, this explanation was not generally accepted until more than 20 years later.

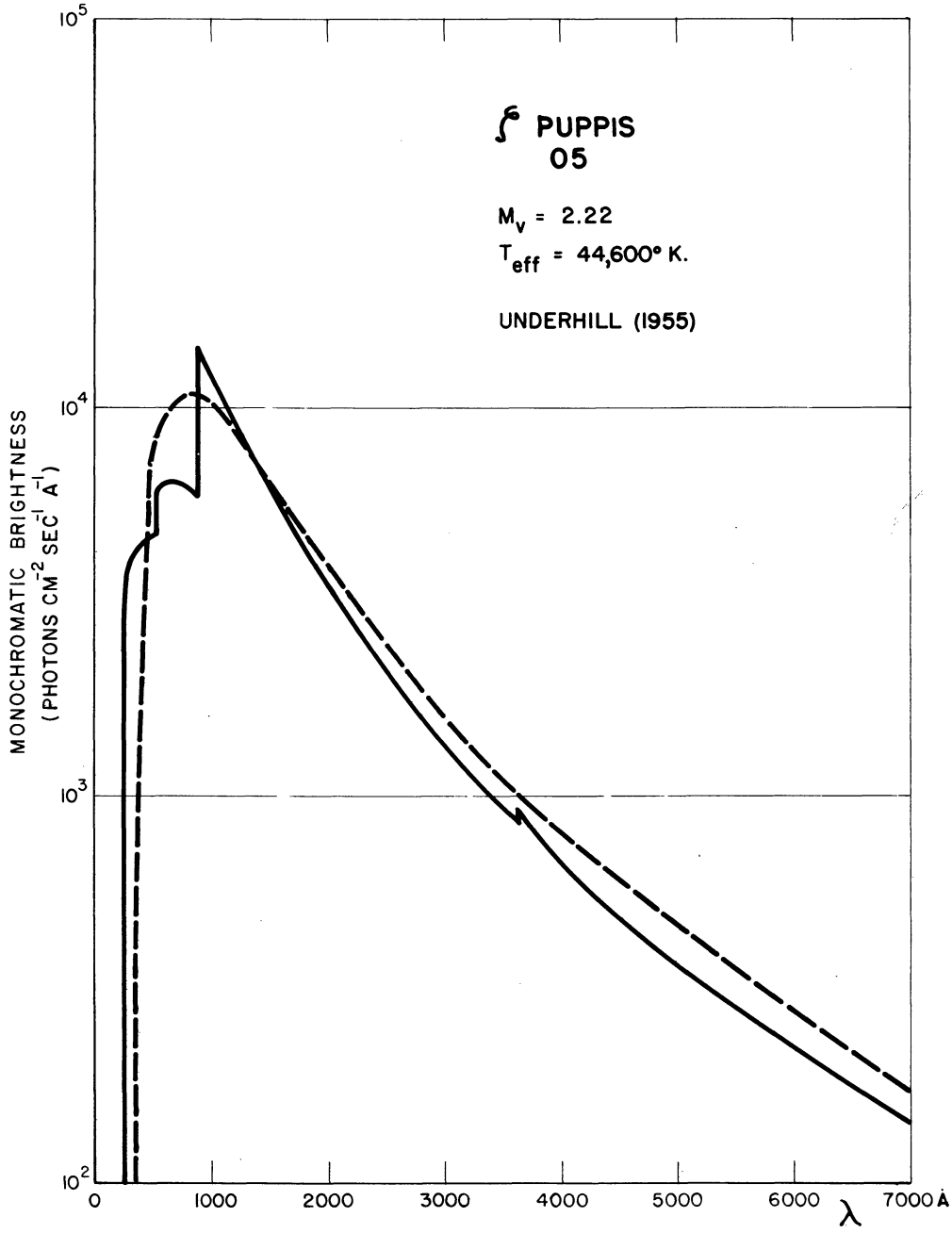

Figures 1A through 1D. --Theoretical stellar spectral distribution curves. **Figure 1A.**

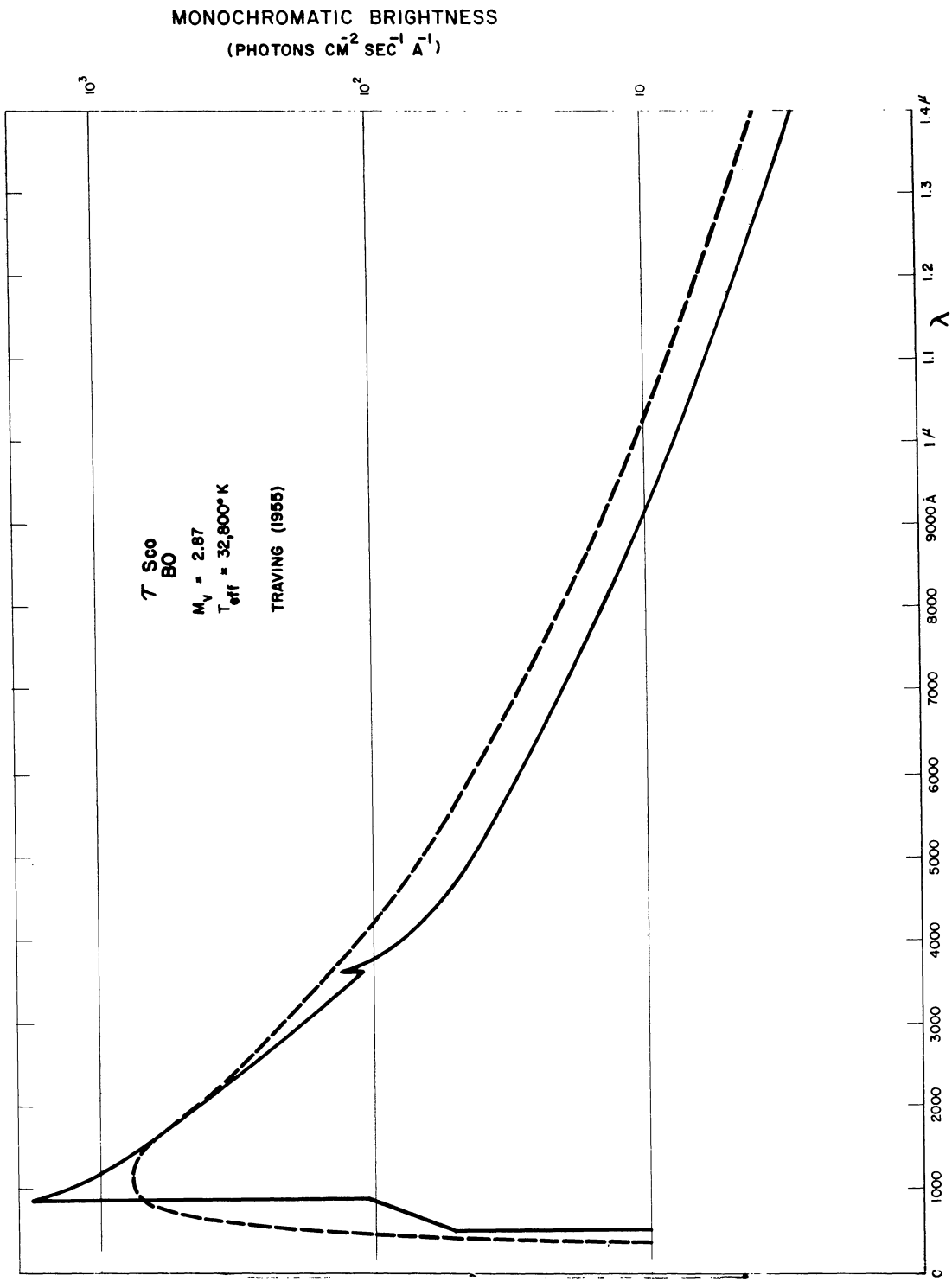

Figure 1B.

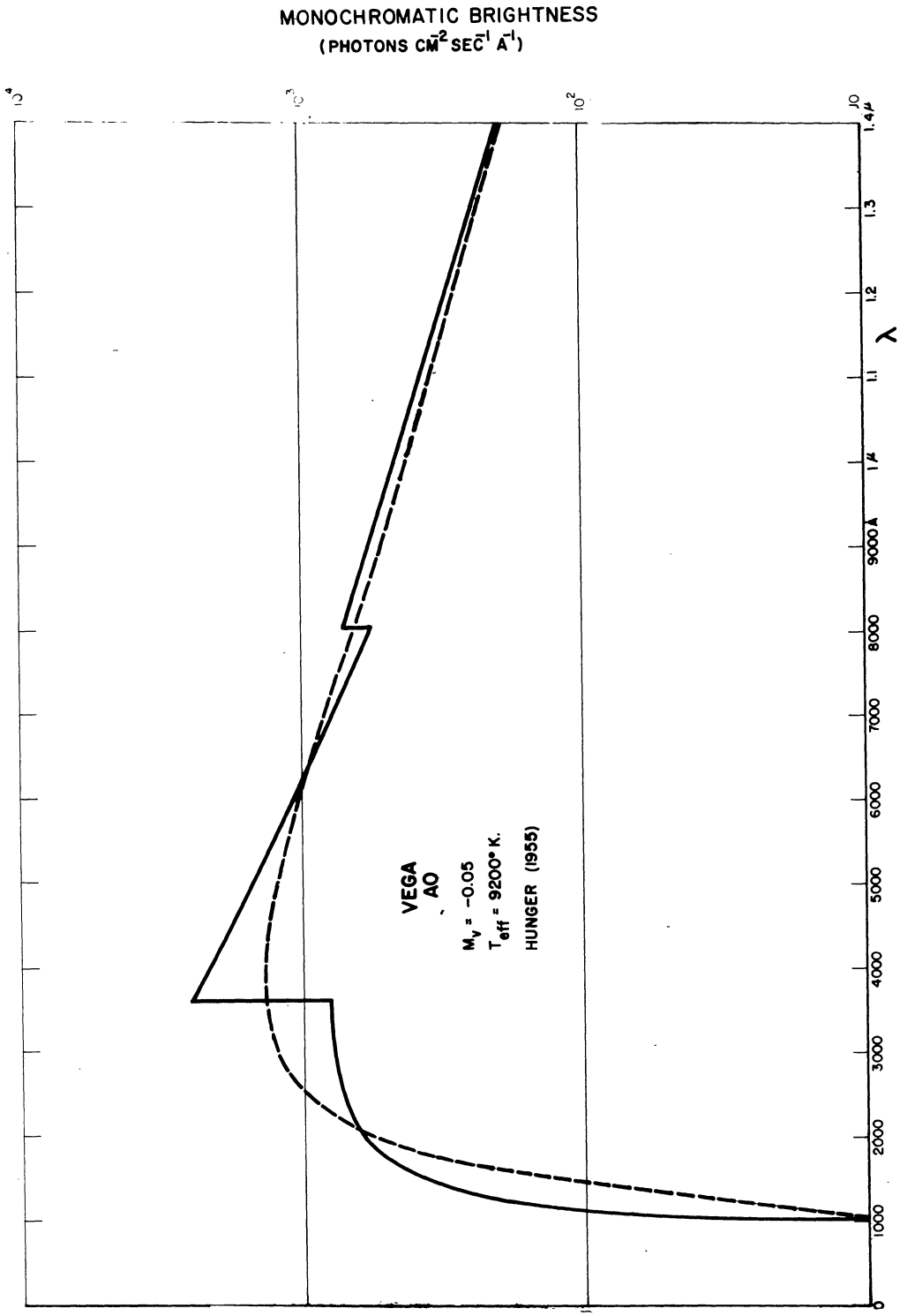

Figure 1C.

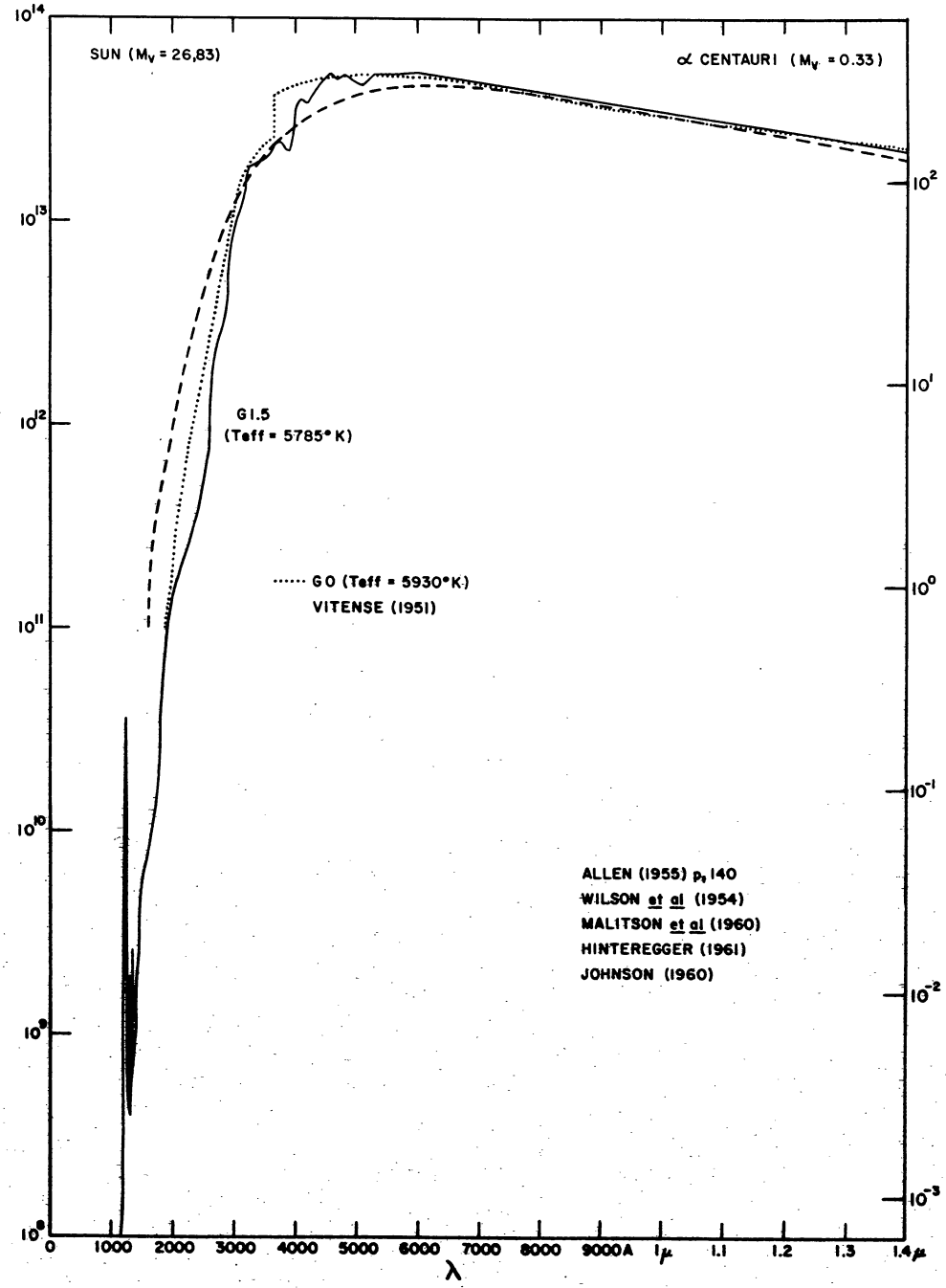

Figure 1D.

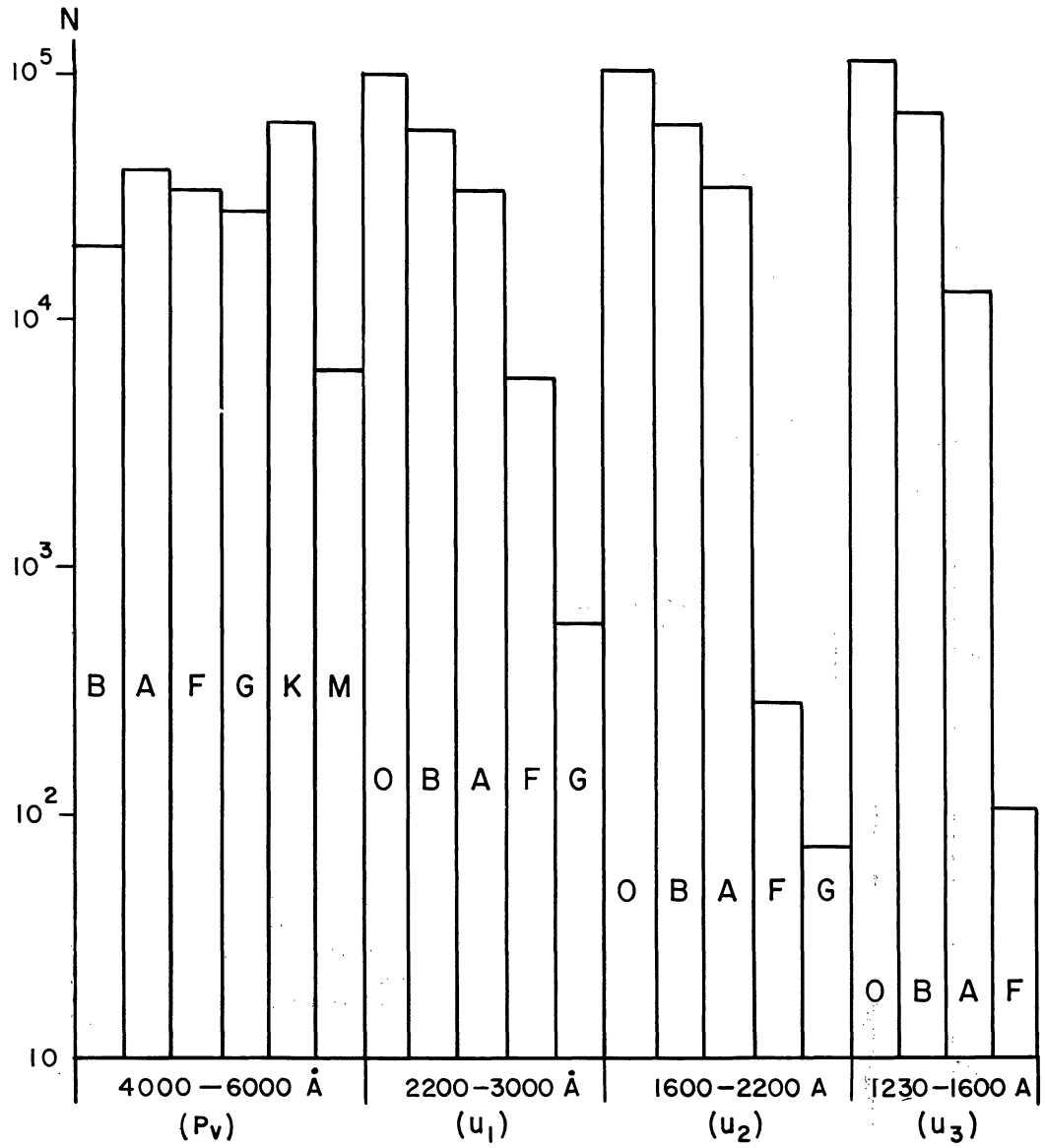

Figure 2.--Number of stars of various spectral types brighter than 9th magnitude in each of four spectral regions.

The absorption spectrum of the interstellar medium is indicated in figure 3. The Lyman-alpha line at 1216 A and most of the absorption between 912 A and 504 A are caused by interstellar hydrogen gas. Since this gas is abundant, no ultraviolet radiation at the Lyman-alpha wavelength or at wavelengths shorter than 912 A can penetrate to the solar system. Thus, we lose very little observational potential by limiting our optical system to 1100 A with the lithium-fluoride faceplate for the camera tube. The x-ray region of the spectrum, where we expect the interstellar medium to open up again, presents optical and astrophysical problems of an entirely different nature not presently the subject of specific planning by Celescope, but discussed in general terms by Baez (1960a, 1960b, 1961) and by Strom and Strom (1961).

The absorption at wavelengths longer than 912 A, except for the hydrogen Lyman-alpha line at 1216 A, is caused primarily by interstellar dust. The region of the curve between 3000 A and 912 A, as yet unobserved, is of importance to the theory of the interstellar dust particles. Celescope will make possible a study of this region. Greenberg (1960) discusses the important question of whether the interstellar dust consists of "classical" particles larger than a wavelength of light, or of "quantum-mechanical" particles of much smaller size.

The interstellar dust also polarizes the starlight passing through it. It is generally agreed that this polarization is caused by elongated particles aligned along or across the lines of force of an interstellar magnetic field. Although Celescope will be unable to measure polarization, future orbiting telescopes will undoubtedly study this important phenomenon in the ultraviolet.

Superposed on the general absorption spectrum shown in figure 3 are several sharp, faint lines caused by atomic and molecular absorption. The study of similar lines in the ultraviolet will be made in the OAO satellite of Princeton University. In the visible region, there are also certain broad absorption features 200 A or so wide, as yet unexplained.

An important part of the reduction procedures for Celescope observations will be to disentangle the effects of the interstellar medium from those of stellar atmospheres.

4. Stars

When plotted in a diagram of absolute magnitude (i.e., intrinsic luminosity) versus effective temperature, the "main-sequence" stars lie along the line indicated in figure 4. In this diagram, the 100 nearest stars are marked by plus signs (+), and the 100 apparently brightest stars by crosses (x). Four stars are common to both groups.

Most of the nearer stars lie on the main sequence. The majority of these, however, are faint red dwarfs that cannot be recognized as such beyond a distance of a few light years. Because most of the apparently bright stars do not lie on the main sequence, and those that do cannot be measured accurately enough, we must rely on the study of physically related groups of stars and on theory to determine the main sequence for spectral types earlier than AO. A major source of error is our inability to separate the components of double stars; known double stars are indicated in figure 4 by circles (O).

To understand the main sequence, we must investigate the evolutionary track of a single star. In some manner as yet very poorly understood, gravitationally stable blobs of matter from the instellar medium lose their excess rotational and magnetic energy to collapse gravitationally. This process continues isothermally until the pressure is great enough so that the gas becomes opaque to the long wavelengths that are carrying off the energy generated. At this point, the temperature

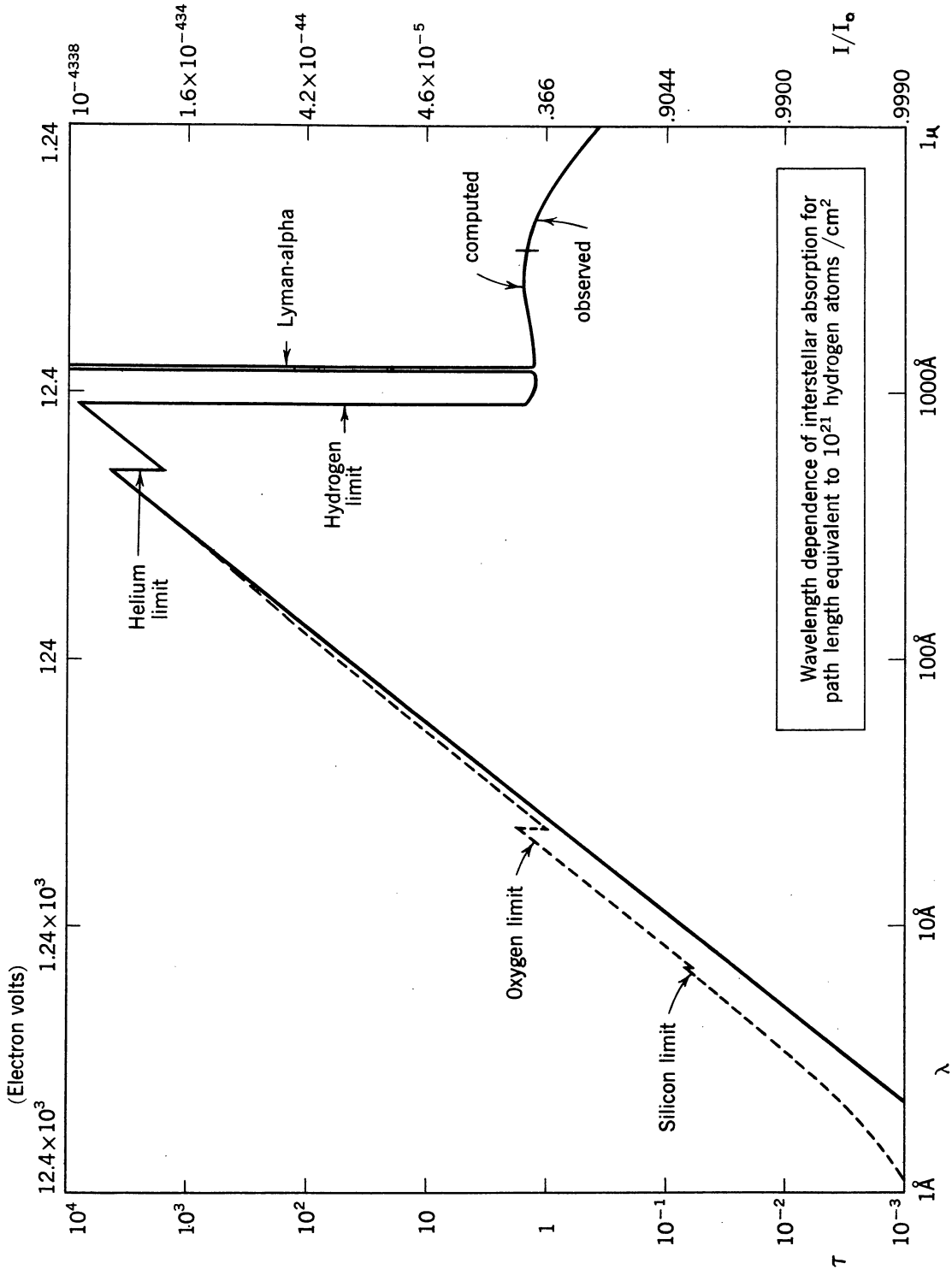

Figure 3.--Wavelength dependence of interstellar absorption for path length equivalent to 10^{21} hydrogen atoms per square centimeter.

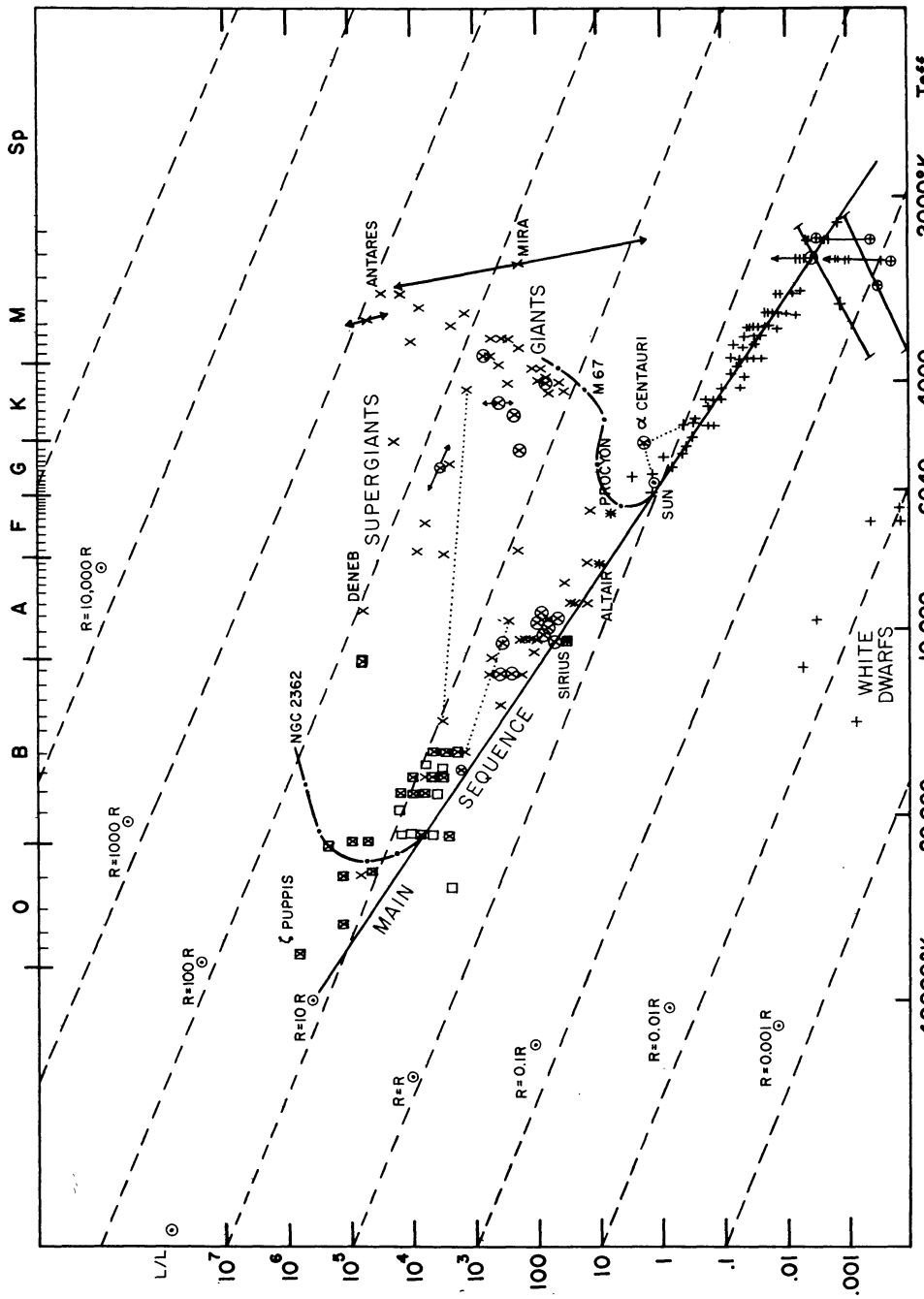

Figure 4.--Luminosity-temperature diagram for stars.

begins rising, rapidly at the center but more slowly at the surface, and the object becomes a star radiating most of its energy in the infrared. As the star contracts, it grows hotter and brighter until the central density and temperature reach a point at which nuclear reactions can occur. If the protostar consists wholly of hydrogen, this point is reached when the central temperature is about 13,000,000° K and the central density is about 83 gm/cm^3. The collapse from protostar to main sequence occupies a very small fraction of a star's lifetime, whereas the release of nuclear energy from the fusion of hydrogen into helium occupies a large fraction of its lifetime. It is for this reason that most stars lie on the main sequence.

A star on the main sequence evolves slowly, moving upward and to the left along the sequence until the supply of hydrogen is exhausted. At that point the star again collapses to release gravitational energy until the central temperature and density become high enough to release nuclear energy by the conversion of helium into carbon. This reaction is much faster than hydrogen-burning, releases more energy per unit time, and thus produces a star of higher luminosity. The higher rate of energy production also causes the outer layers of the star to expand. Such a red giant has lower surface temperature and greater total luminosity than the main-sequence star from which it evolved.

After the helium-burning stage, evolution again proceeds very rapidly, ending with the star's collapsing to the white-dwarf stage. Because its nuclear fuel is spent and its surface area is small, the white dwarf releases its stored thermal energy slowly.

The position a star occupies while it is on the main sequence depends upon its mass, the more massive stars being hotter and brighter than the less massive. As figure 4 indicates, most stars are red dwarfs. Because of selection effects, however, most of the apparently bright stars are the hotter main-sequence stars and the red giants. When we observe in the ultraviolet, we favor even more strongly the hot stars. This is also evident in figure 4, in which the 27 theoretically brightest stars at 1250 A are indicated by squares (□).

Thus with Celescope we expect to observe primarily stars with effective surface temperatures in excess of 10,000° K. What of the other stars? If the sun is typical of the cool main-sequence stars, we would observe the chromospheric radiation from a handful of G stars (including Alpha Centauri) in the 2200 to 3000 A band. We might conjecture that the red giants have exaggerated chromospheres, and that we would observe the ultraviolet radiation from some of them. The white and red dwarfs would almost surely not be detected at all. If, however, the flare stars have flares similar to those on the sun, we might detect the ultraviolet radiation from some of them. Flare stars are red dwarfs that occasionally, for periods of a few minutes, increase their luminosity especially in the yellow and blue regions of the spectrum, by factors from 10 to 100. They are indicated in figure 4 by vertical arrows proceeding upward from their symbols.

Several Wolf-Rayet stars will almost certainly be prominent on the Celescope survey. Their spectra consist almost wholly of bright lines and bands. Their effective surface temperatures are not well known. Their surface temperatures as indicated by ionization and excitation effects are comparable to or greater than the effective surface temperatures of the O stars. Figure 4 includes only one Wolf-Rayet star, Gamma Velorum.

The central stars of the planetary nebulae are similar to the Wolf-Rayet, but are intrinsically about 3 magnitudes (i.e., a factor of 16) fainter. Many of them are expected to show up in the Celescope survey. Only the nearer planetary nebulae have angular dimensions large enough for the Celescope to be able to separate the ultraviolet radiation of the central star from that of the nebula.

Novae and supernovae would certainly be interesting objects to observe in the ultraviolet, should any flare up during the course of the Celescope survey. In a nova outburst, a star's light increases by about 12 magnitudes (or a factor of over six million times), and the star sheds a fraction of one percent of its mass. The nova stage is apparently related to the evolution of a star of moderate mass from the red-giant to the white-dwarf stage.

In a supernova outburst, a star loses several percent of its mass, a truly catastrophic process. Type I supernovae are old stars that have too high a mass to allow them to change gracefully from red giant to white dwarf. When the nuclear fuel in the core is exhausted, the star collapses, heating up the nuclear fuels in the envelope to create a gigantic fusion bomb. The neutrons released in this explosion build up heavier elements from the core materials, beginning primarily with iron. The light curve of this type of supernova exhibits the same half-life as Californium-254, leading some authors to the hypothesis that a large amount of this isotope is generated in the supernova explosion. A Type I supernova has a peak intensity about 18 magnitudes brighter than that of the star before the outburst.

Type II supernovae must be young stars, since they are found only in those parts of galaxies where star formation is occurring. Blaauw (1961) describes a new theory that explains these objects as the explosions of protostars too massive to become stable stars.

Both types of supernovae are very rare objects, none having occurred in our own galaxy since the invention of modern photometric and spectroscopic techniques. They are, however, bright enough so that Celescope might be able to observe one should it occur in one of the nearer external galaxies. Novae are more common.

Many other types of peculiar stars might be especially interesting for Celescope, such as the P-Cygni stars and a group of peculiar A stars that includes the magnetic and spectrum variables.

5. Nebulae

In the interstellar gas and dust there occur concentrations, or nebulosities. Of special interest to Celescope are those gaseous nebulae that shine because of fluorescent excitation by early-type stars embedded in them. One category of such nebulae is represented by the Great Nebula in Orion, which is excited by the group of O stars called Theta Orionis. With Celescope's limited angular resolving power we will not be able to resolve the details of their structure as we could do in visible light from a large earth-based reflector; from our slitless spectroscope, however, we will be able to identify the ultraviolet lines excited in the spectra of some of the smaller nebulae.

A second category is the planetary nebulae, smaller and more regular in shape than the diffuse nebulae. Under low magnification, many of them resemble planets. They are created by the expulsion of matter from their hot, rather strange central stars, and rather rapidly expand and dissipate in interstellar space. The ultraviolet spectra of these objects are also of interest to Celescope.

Photometry of the diffuse and planetary nebulae with Celescope's broad-band television equipment will probably not be particularly useful; we must, rather, rely on the slitless spectroscope in our study of these objects. Since their spectra consist primarily of emission lines, and since most of them are expected to appear as point objects at Celescope's resolving power, we expect to be able to obtain spectra of the brighter nebulae.

A third category of nebulosity, of special interest to the astrophysicist and galactic astronomer, is the molecular-hydrogen (H_2) region. At least 90 percent of the matter in interstellar space is hydrogen gas. At present, we can study atomic hydrogen (H I) regions by means of radio astronomy at 21 centimeters, and ionized hydrogen (H II) regions by means of optical astronomy at the H-alpha line (6563 A). There are no techniques in the presently available regions of the spectrum to study possible interstellar clouds of molecular hydrogen. There are several indications that such clouds exist, including indirect deductions from radio-astronomical data, and the discovery of ultraviolet nebulosities by means of rocket-borne detectors (Kupperian, Boggess, and Milligan, 1958). Dr. Max Krook, of Harvard College Observatory, has suggested that this radiation is caused by Raman scattering of Lyman-alpha radiation by molecular hydrogen. If so, the ultraviolet nebulosities radiate monochromatically at 1284 A and at 2.38 microns. We are now attempting to detect the 2.38-micron radiation, should it exist, from the ultraviolet nebulosities observed in Orion and Virgo. It should be pointed out that other authors (Shklovskii, 1959; Pikel'ner et al., 1959; Hayakawa, 1959; Scientific American, 1960) ascribe this radiation to other causes.

Celescope may also be sufficiently sensitive to allow us to study the ultraviolet radiation from molecular-hydrogen regions. It is unfortunate, however, that except for the possible Raman line at 1284 A, the primary spectral lines of molecular hydrogen all fall below 1150 A under the anticipated interstellar conditions.

6. Galaxies

All of the objects discussed up to this point are members of our own Milky Way galaxy, and because of interstellar absorption we expect most of them to lie within a few thousand light years of the earth.

Celescope is not specially designed to observe external galaxies, which according to most reasonable theories will not be bright enough in the ultraviolet for proper study. As was the case with radio astronomy, we might discover that some peculiar galaxies are bright sources for our new wavelength region.

Among peculiar galaxies of special interest in this regard are the radio sources Virgo A and Cygnus A. The first (M87) is an elliptical galaxy possessing a luminous jet. The light from this jet is polarized and may be generated by synchrotron radiation. Cygnus A, although the second-brightest radio source in the sky, is optically rather faint. Originally interpreted as a pair of colliding galaxies, it is now more commonly claimed to be a single galaxy with a rare, although not unique, peculiarity.

7. Solar System

The most important, most interesting, and most studied body in the solar system (excluding the earth) is the sun. Because of its great brightness, the sun will not be observed by Celescope, since equipment suitable for its study cannot be used for study of any other body. Ultraviolet study of the sun is, however, of special interest to Celescope, since at present the sun is the only star that has been well observed in the ultraviolet. Our knowledge of the sun's radiation can serve to guide us in our design studies.

Figure 1 shows the measured continuous spectrum of the sun. Below 1500 A, the major portion of the energy is contained in the emission-line spectrum rather than in the continuum. However, at these short wavelengths no other star similar to the sun would be bright enough to be observed. If we are to observe any stars of G and later spectral type with Celescope, we will truly be probing the unknown and unexpected--the most exciting part of science.

The sun's ultraviolet radiation comes primarily from the chromosphere, a layer of tenuous gas lying above the visible solar surface. The chromosphere is raised by mechanical agitation to a temperature approximately twice that of the visible surface, or photosphere. Just below the photosphere, the sun is in a boiling, bubbling state of convective energy transport. In and beyond the photosphere, the primary energy transport mechanism is radiation rather than convection. However, the momentum carried by the convection is transported through the photosphere into two regions, the chromosphere and corona, where the gas density is so low that thermodynamic equilibrium no longer holds even approximately. The temperature as expressed by the kinetic energy of the electrons, ions, and atoms--i.e., the electron temperature T_e--rises in the chromosphere to 10,000° K., whereas the radiation temperature falls below the 5785° value maintained just below the photosphere where the gases cannot "see" the cold of outer space. And since the overlying gases are hotter than the photosphere, the ultraviolet picture of the sun will be brightest at wavelengths where those gases are opaque, thus causing the far ultraviolet radiation of the sun to be generated primarily in the chromosphere.

The sun is continually expelling clouds of particles. Optical evidence of this activity is furnished by the prominence photographs being taken at the world's great solar observatories. Such clouds carry ions, electrons, and magnetic fields. These particles and fields interact with the earth's atmosphere and magnetic field to produce ionospheric disturbances, magnetic storms, and aurorae.

The earth's upper atmosphere interacts not only with the solar corpuscular but also with the electromagnetic radiation. Rocket observations have shown that both the daytime and nighttime skies are strong emitters of Lyman-alpha radiation (Kupperian, Byram, Chubb, and Friedman, 1958). The daytime illumination indicates that the earth's outer atmosphere reflects 70 percent of this radiation. The mechanism is resonant scattering by neutral hydrogen atoms. The nighttime illumination, which is much fainter, is caused by recombination of ionized hydrogen. This hydrogenic component of the atmosphere fades into the interplanetary gas, which, being composed of hydrogen, is also bright in Lyman-alpha. Lyman-alpha is not the only ultraviolet line to be expected in the spectrum of the upper atmosphere. Oxygen, nitrogen, and carbon compounds will also be strong emitters.

Ultraviolet radiation is also to be expected from other planetary atmospheres. However, the Lyman-alpha component is expected to be masked by the interplanetary background, and the longer-wavelength components may be too faint to be detected with Celescope.

II. Experimental Objectives

1. All-sky Survey

The original and still primary objective of the Celescope program is to obtain ultraviolet maps of the sky in one or more colors below 3000 A to serve as the basis of further studies with more advanced satellites. Our goal, as presently stated, is to obtain all-sky maps in three ultra-

violet colors to a limiting magnitude* of 10.0 for stars, and to a limiting sensitivity for nebulae sufficient to give rather detailed pictures of the ultraviolet nebulosities discovered by Kupperian, Boggess, and Milligan (1958). The stellar limit should provide us with data on about 100,000 stars, virtually all of which are expected to be F-type or earlier. The nebular limit corresponds to about 12th magnitude per square minute of arc, or 10^{-5} photons sec^{-1} cm^{-2} $Angstrom^{-1}$ $(minute\ of\ arc)^{-1}$, or 5×10^{-10} erg sec^{-1} cm^{-2} $Angstrom^{-1}$ $steradian^{-1}$.

The nebular maps and the stellar maps pose entirely different sets of problems. Since our stellar sensitivity requirements are relatively modest, we can concentrate on improving resolution in position and intensity measurements. We are designing our equipment to give a position resolution of 30 seconds of arc, and an intensity resolution of 0.1 magnitude. Our stellar information is contained in only a few picture elements, 1000 or fewer even in the most crowded regions of the sky. By concentrating on the stellar images and disregarding any information not contained in them, we are able to handle the stellar television photometry entirely in digital form, easily allowing us to retain the resolution capabilities of the camera tube throughout the data-handling system. These capabilities allow us 9 bits of positional accuracy in both the horizontal and vertical directions, and 7 bits of intensity accuracy. For these stellar pictures, the satellite data-handling system treats nebulosities as "noise" that is filtered out prior to transmission to the ground, and no bandwidth is required to describe the "black" areas between the stars.

The nebular pictures require that we increase sensitivity at the expense of both angular and intensity resolution. We can make no valuable a priori assumptions regarding the information content of the picture, as we were able to do in the case of the stars; and because our signal transmission bandwidth is limited to 62 kc/sec, we can no longer use digital techniques. To maximize our sensitivity, we will use the longest exposure time readily available--probably 30 seconds--and go to our minimum acceptable resolution by using a scanning beam with large cross-section. We anticipate a resolving power of about 2 to 4 minutes of arc, and an intensity resolution corresponding to about 20 shades of gray. The picture will be transmitted by analog techniques.

The nebular pictures will be recorded by photographic (kinescope) techniques. The pictures will be studied both directly and photometrically, and will be used to create the maps that will be published. The stellar pictures will be analyzed directly by a digital computer to construct a star catalog similar to the Henry Draper catalog in format and amount of information. This catalog will then be published for further study and analysis.

The observations will be ordered in such a way that an early failure of the satellite will still leave us with data having the greatest possible statistical value. Our first observations will cover rather thoroughly the constellation of Orion (the OB association Orion I). We will then study a set of "selected areas", going from one area to another in a predetermined fashion. Some of these areas will be on the galactic equator, and others will be far from it. Finally, we will fill in the remaining portion of the sky in the most efficient manner.

2. Slitless Spectra

In addition to the broad-band photometers, we plan to install a slitless spectroscope in the Celescope. Because of the small field of view of our detector, our spectra will extend only 0.5

---

* A star of 10th magnitude in the ultraviolet delivers the same ultraviolet flux as does an AO star of photographic magnitude 10.0.

inch between the wavelength limits of 1100 A and 2200 A. This short length will allow most spectra to appear in their entirety on one picture, since there is 0.1 inch of overlap between adjacent pictures. We have used our Type B sensitivity to limit the observed spectral region so as to prevent interference from overlapping spectral orders.

Our resolving power, limited by the scanning raster of the detector, will be about 8 A. With the stellar spectra spread out like this, our limiting magnitude will be about 6.0, giving us an expectation of about 5,000 stars. The total information content, however, as measured by the number of binary words required to describe our pictures, will be approximately the same as for one of the broad-band television photometers.

The slitless spectroscope will thus enable us to plot the continuous spectra of the brighter stars through about 100 points, whereas the broad-band equipments will enable us to plot the continuous spectra of a much greater number of stars through three points. The two techniques are complementary, the detailed study of individual stars supplementing a less accurate survey of a large number of stars.

3. The Solar System

As mentioned above, Celescope will not be used to study the sun. The OAO spacecraft is programmed so that the optic axis will never come within 45° of the sun, and a sun shield should close to keep the direct rays of the sun from entering the Celescope tube should this limit be passed. Direct solar illumination would destroy the detector.

The earth's atmosphere is expected to be a strong and interesting source of ultraviolet radiation that Celescope may well be suited to study. We plan to look downward at both the illuminated and dark portions of the atmosphere. An intensive study will be made only if it does not interfere with the celestial observations, or if Celescope proves unsuccessful in its celestial mission. Looking upward, we expect to find no atmospheric emission or absorption other than the Lyman-alpha emission at 1216 A.

The other planets are not expected to be bright in the ultraviolet, but Celescope will definitely look for them, and surprises are to be anticipated. The slitless spectroscope may show some of them as Lyman-alpha emission objects, if they are intense enough to shine through the general background radiation.

We will also make a special effort to observe the interplanetary medium. Scattered Lyman-alpha radiation will fall within the detection band of our slitless spectroscope, and thus be subject to study. By observations made near the sun when direct sunlight is blocked by the earth we hope to be able to observe clouds of gas expelled from the sun. These observations would complement those now being made of the effects on the earth's magnetic field and ionosphere of clouds of ionized particles expelled by the sun.

4. Objects of Special Interest

We anticipate that many objects of interest will not be detected on the sky survey. We are now compiling a list of special and peculiar objects that would be of interest even if they are below the threshold of Celescope's normal operation. Since the slewing capabilities of the spacecraft will not allow us to use the entire communications contact time, we will be able to take additional long exposures on regions containing these objects. Among such objects will be

the radio sources 3C48, Cygnus A, Virgo A, and Taurus A; selected OB associations such as Perseus II that are near enough and uncomplicated enough for convenient study; a few selected planetary nebulae; a selection of Wolf-Rayet stars; and additional classes of objects too numerous to mention here.

5. Calibration Techniques

Proper calibration of the Celescope is so important that we anticipate spending as much as half of our entire effort to ensure proper calibration of adequate quality. Our techniques for the calibration of the various Celescope components are growing to keep step with the camera-tube development program. Although the spectral response and the sensitivity of each tube are calibrated by the manufacturer, we recheck all tubes when we receive them and again when they are mounted in prototype and flight equipment. Figure 5 is a photograph of our calibration equipment.

We begin by calibrating a hydrogen-arc ultraviolet source. This lamp is placed at the entrance slit of a vacuum monochromator, and a nitric-oxide photon counter is positioned at the exit slit. The monochromator is set to isolate the Lyman-alpha radiation of the lamp. We know the efficiency of the counter from the absorption cross-section of nitric oxide at this wavelength. This arrangement gives the absolute flux of Lyman-alpha emerging from the exit slit.

We now replace the nitric-oxide detector with a photomultiplier tube coated with sodium salicylate. The fluorescent quantum efficiency of this material is constant over the spectral range of 1000 to 3500 A. By scanning the monochromator through this range, we obtain the relative spectral output curve of the monochromator under our standard calibration-scanning conditions. The absolute output is determined from the response at Lyman-alpha.

We next check this calibration by means of a thermocouple. We first take a spectral scan using the hydrogen source and a thermocouple detector. Then we calibrate the thermocouple against a standard incandescent lamp certified by the Bureau of Standards. We resolve any disagreement between these two independent methods before proceeding to the next step.

For calibrating a television camera tube, we place the tube at the exit slit of the monochromator and scan the spectrum in the standard manner. We record the video output on an oscilloscope to obtain the video output signal as a function of wavelength and position on the faceplate of the tube. Since the exit slit will be .05 x 8 millimeters and the photocathode is used over a 25-mm square area, this mapping of the spectral sensitivity of each tube is a time-consuming operation.

The calibration is not complete until the other elements of this system, and the assembled system itself, have been calibrated. To measure the reflectivities of our mirrors, we coat a small test-plate when we coat each mirror surface. A special attachment at the exit slit of the monochromator allows us to measure in quick succession the direct and the reflected beam. We can thus determine the effect of mirror reflectivity on our system response. The same apparatus allows us to measure the transmissivity of each optical filter.

We can calibrate our electronic systems (video amplifiers and communication link) by impressing electronically generated video-signals of known amplitude at the signal input electrodes.

Figure 5.--Celescope spectrophotometric calibration equipment.

For the system test, we must go to the vacuum optical bench to be built at NASA'a Goddard Space Flight Center for OAO use. Its ultraviolet source must be calibrated by means similar to those used on our equipment. If the system calibration does not agree with the sum of the calibrations of the parts, we must again look for and remove the sources of error.

It is highly important to protect all of our optical elements, i.e., mirrors, filters, and detectors, from any environment that would tend to change the system's spectral response curve, since once the Celescope is assembled, re-measuring these quantities to the desired accuracy becomes very difficult, if not impossible. After assembly of the Celescope we will, therefore, rely on calibrated point sources to check the sensitivity calibration. Once the satellite is in orbit, it may be impossible to differentiate between sensitivity changes caused by the optics and those caused by the electronics.

Our satellite-borne calibrator will consist of an artificial star generator (see fig. 7) to focus a spot of known spectrum and intensity onto the photocathode. The response of the system to this signal will enable us to determine system sensitivity changes. We also have portable ultraviolet spot generators to be used as necessary during assembly of the Celescope. Once assembly is complete, we will, of course, be able to use the ultraviolet calibrators to maintain our sensitivity calibration through subsequent fabrication, countdown, and launch. This calibration will be independently checked, in the Goddard Space Flight Center vacuum optical facility, as close as possible to final assembly of the OAO.

Each step in the calibration is performed as near as possible to the time of the first observation. By making our first observations in Orion, where there is a large number of stars expected to be bright in the ultraviolet, we hope to locate early a field suitable as a photometric standard. We will then return to that field frequently while we set up secondary standards. We will observe some standard field at least once per day, and use the internal calibration at least twice per orbit. Thus, we will be using our artificial standard as an aid to interpolation only. The calibration sequence will be varied as necessary during operation.

6. Stellar Distribution and Speed of Completion of Survey

Davis and Godfredsen's (1961) study of the relationships between stellar distribution and Celescope data-handling requirements led to the results given in figure 2. This study used model stellar atmospheres published before 1958, and may therefore have overestimated the ultraviolet brightnesses of the hotter stars. (See p. 3, above.) Although this study was aimed mainly at the problem of information loss caused by the presence of accidental double stars, it now appears that the most important result was that pertaining to the distribution of the ultraviolet stars. For our anticipated resolving power of 30" of arc, we expect only about one percent of our objects to be unresolved double stars. This percentage is very nearly proportional to the square of the angular resolution.

If we achieve our target sensitivity, and if the stars have their predicted brightnesses in the ultraviolet, our three all-sky broad-band ultraviolet maps will contain about 100,000 stars. Our field of view will be $2^{\circ}.4$ square (see below), so that each picture will cover 1/7220 of the sky. The average picture will therefore contain 14 stars. However, an average picture in the galactic plane will contain about 80 stars, and the densest fields may contain 250. Figure 6 shows the expected distribution in galactic latitude of stars observed at various wavelengths.

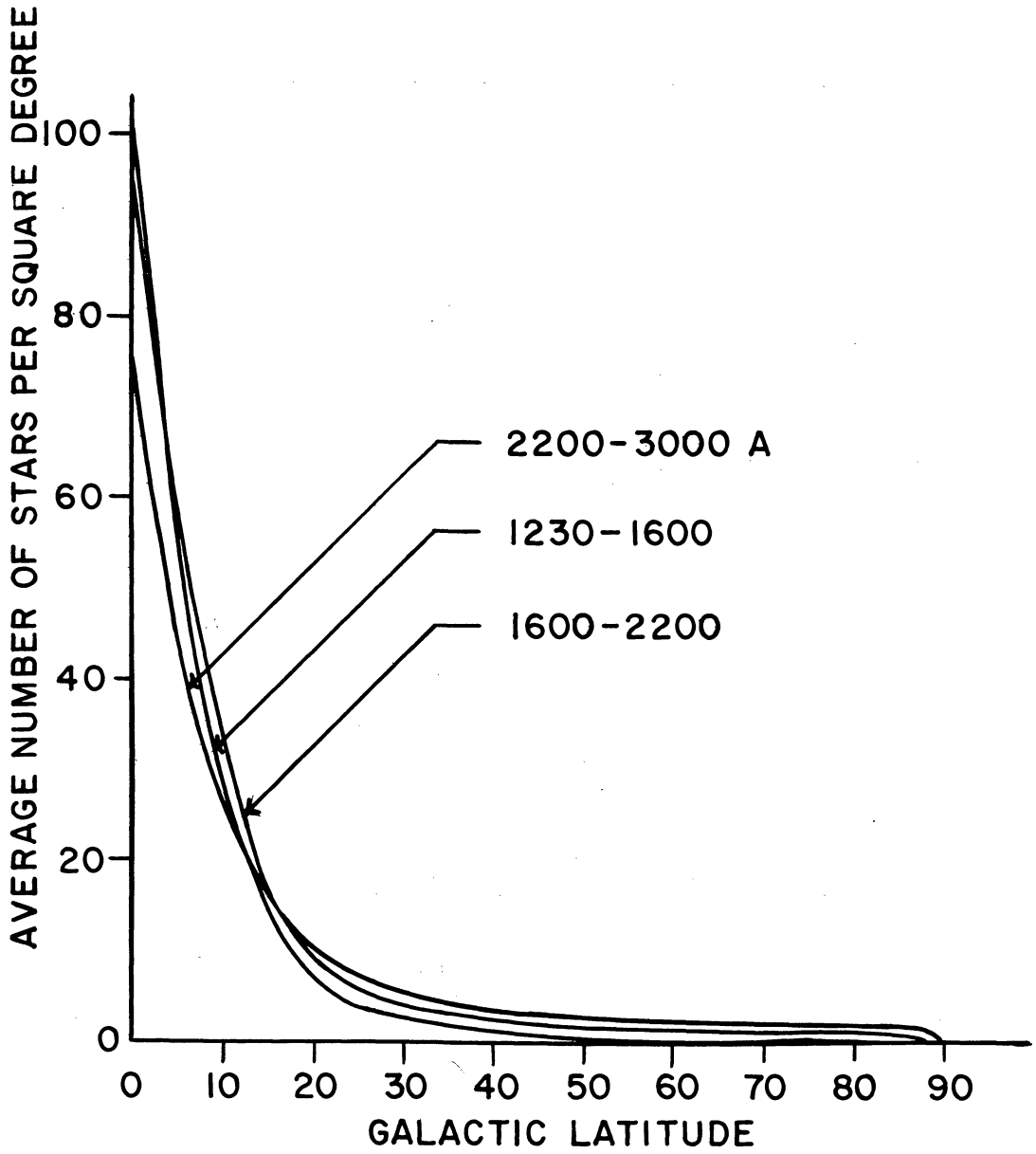

Figure 6.--Average number of stars per square degree as a function of galactic latitude and of wavelength.

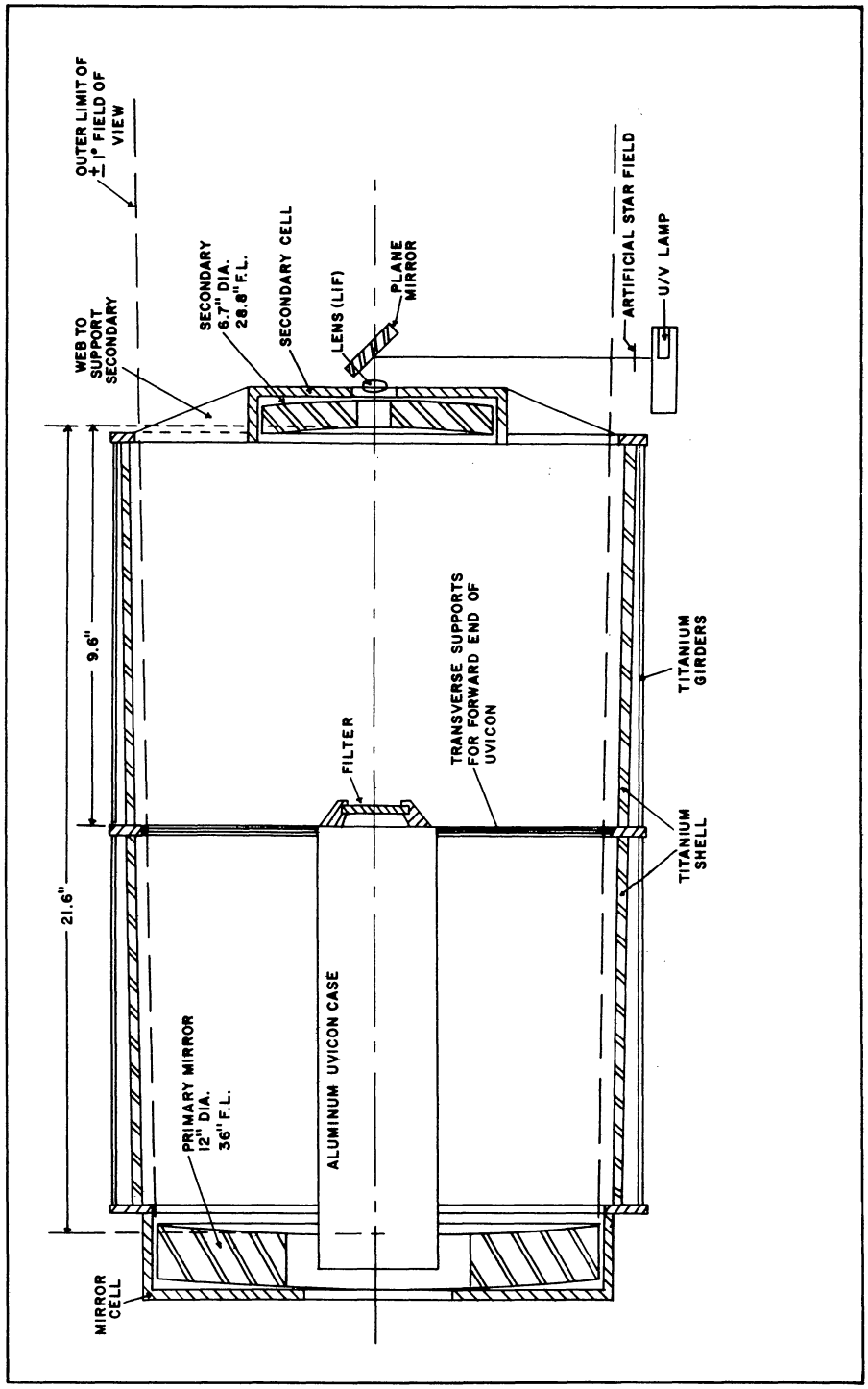

Figure 7.--Schwarzschild camera for Celescope.

In any field, 60 percent of the stars are expected to be at threshold. An average star will occupy four elementary areas of the television scan, and will therefore require four binary "words" to describe it.

In order to provide a margin of safety, our centers will be separated by $2^{\circ}.2$ rather than $2^{\circ}.4$. We would thus require 8520 slews of $2^{\circ}.2$ each to cover the entire sky. We are allowed an average of four such slews per orbit. However, transfer between the University of Wisconsin and the Smithsonian experiments and slewing to standard fields for calibration will probably limit us to a working average of three slews per orbit, corresponding to 42 fields per day. It is rather optimistic to hope that we will be able to achieve better than 50 percent efficiency in our actual operation. Our anticipated time for completion of the program is therefore 400 days.

III. Experimental Instrumentation

The entire Celescope system has been built around the television camera tube that we use as a detector. At the start of the program in 1959, television had never been successfully used in either astronomical or ultraviolet research. Our expectations for Celescope's accuracy and reliability still far exceed anything that has since been done with television, even in ground-based observatories and laboratories. Our first step in this program was to initiate the development of a television camera-tube that could be used in Celescope. After this tube had been developed to essentially its final configuration, we designed an optical system around it. As the last step, we are now designing the mechanical system to hold the optical elements in place, and the electronic system to operate Celescope's television cameras by remote control from the ground. Figure 7 shows the system as we presently contemplate it.

1. Sensory System

Since optical filters alone cannot isolate the spectral regions of interest to Celescope, we require a different type of television camera tubes for each color. The Westinghouse Research Laboratories have developed these tubes for us. Figure 8 shows preliminary spectral response curves for the three types. Type A operates at an effective wavelength of about 2200 A; Type B (plus the barium-fluoride filter) at about 1500 A; and Type C at about 1350 A. Under Celescope operating conditions, these tubes will have a threshold about equivalent to the radiation received from a 10th magnitude star: 3500 photons per second in a point image within the spectral pass band.

Our requirements for sensitivity and spectral response can be stated mathematically as follows:

$$\int_{\lambda_1}^{\lambda_2} S_\lambda \, d\lambda \geq 10 \text{ photons cm}^{-2} \text{ sec}^{-1} \text{ (resolution element)}^{-2} ;$$

$$\int_0^{\lambda_1} S_\lambda \, d\lambda \leq 10^{-4} \int_{\lambda_1}^{\lambda_2} S_\lambda \, d\lambda \geq \int_{\lambda_2}^{\infty} S_\lambda \, d\lambda ,$$

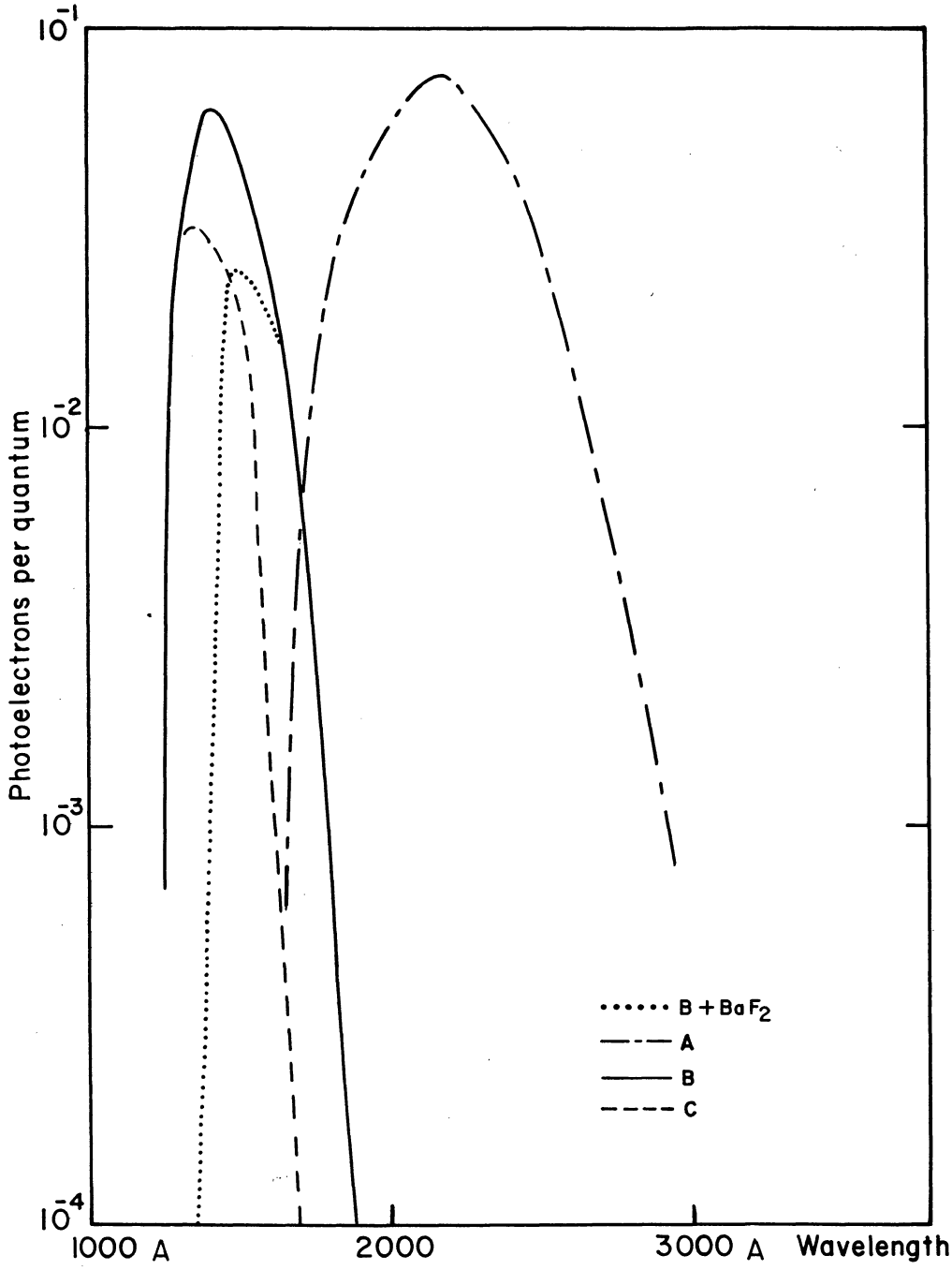

Figure 8. --Preliminary response curves of three types of ultraviolet-sensitive ebicons.

where S_λ is the system sensitivity in photons per resolution element per square centimeter per second per Angstrom unit; and λ_1 and λ_2 assume the following values:

	λ_1	λ_2
Type A	2000 A	3000 A
Type B	1100 A	2000 A
Type B + BaF_2 filter	1500 A	2000 A
Type C	1270 A	1500 A

The tolerances are ± 200 A, except that for types C and B, λ_1 is ± 50 A.

With an optical system of 12-inch aperture, this requirement can be restated:

$$\int_{\lambda_1}^{\lambda_2} S_\lambda d\lambda = 3500 \text{ photons sec}^{-1} (40\mu)^{-2} .$$

The Westinghouse Type B detector now appears to have this sensitivity with one-second integrating time, λ_2 = 2300 A, and λ_1 = 1100 A. In the Celescope, we will change λ_1 to about 1500 A by inserting a suitable optical filter. We will, of course, measure λ_1, λ_2, and S_λ for each Celescope system as accurately as possible during the preflight calibration.

A telescope of effective focal ratio T/3.7 would be able to detect, at threshold for one-second exposure, nebulae of intensity 8 x 10^{-3} erg sec^{-1} cm^{-2} $steradian^{-1}$, which is equivalent to 20 photons sec^{-1} cm^{-2} (30" of arc)$^{-2}$. The brightest nebula observed by Kupperian, Boggess, and Milligan (1958) is one-third of this threshold; their Spica nebulosity is one-sixth of this value. For our 30-second exposures at one-fourth the stellar resolving power, we therefore expect our threshold to be 13 db below this observed value for the Spica nebulosity.

The dynamic range for the stars is expected to be about 5 x 10^4 above the threshold of 10 photons sec^{-1} cm^{-2} for point sources. For the nebulae we expect a much smaller dynamic range of about 40. For the stellar television photometers we are striving for an accuracy of 0.1 magnitude, requiring somewhat less than 128 (i.e., 2^7) discernible levels. For the nebular television cameras, however, we need only 20.

We have not yet determined the maximum usable integrating time for one of these detectors. Some vidicons have been produced, however, for which integrating times above 1000 seconds still give improvement in sensitivity. We have proved that total exposure is still proportional to exposure time between 0.03 and 30 seconds.

The simplest tube capable of meeting our sensitivity requirements appears to be the ebicon. Because of the high importance of simplicity, we have chosen that design. Skorinko et al. (1961) have described the resulting Westinghouse uvicon, which is illustrated here in figure 9.

The front section of the uvicon is an electron-imaging section. Photoelectrons from the photocathode are accelerated through 15 kilovolts and focussed onto the ebic target, the resulting electron image being one-half the size of the initial optical image. This target, named for its operation by electron bombardment induced conductivity, becomes conductive at those points where it has been bombarded by high-energy electrons, allowing a charge pattern to build up that contains about 300 image electrons for every bombarding electron. The back section of the tube is an electron gun used for reading the target in exactly the same manner as for a vidicon.

The photocathode determines the spectral sensitivity of the camera tube. The Type A uvicon uses a photocathode of caesium telluride with a conducting substrate of nickel deposited onto a lithium-fluoride faceplate. Since caesium telluride is destroyed by air, this type of photocathode must be created inside the tube after evacuation. The long-wavelength cutoff is determined by the photoelectric response of the caesium telluride, and the short-wavelength cutoff is determined by the transparency of the nickel substrate. For Celescope we may mount a quartz window in front of the Type A uvicon to limit further the short-wavelength response.

The Type B uvicon uses a photocathode of caesium iodide with a conducting substrate of palladium deposited onto a lithium-fluoride faceplate. Again, the long-wavelength cutoff is determined by the photoelectric material, and the short-wavelength cutoff of the tube by the transparency of the conducting substrate. However, for Celescope, we will mount a barium-fluoride window in front of the Type B uvicon to limit the short-wavelength response.

The Type C uvicon is similar to the Type B, except that the photoelectric material is barium-fluoride. We will mount a calcium-fluoride window in front of the Type C uvicon to limit the short-wavelength response. Neither Type B nor Type C photocathodes are harmed by exposure to air during construction of the tube.

Figure 8 shows preliminary response curves of these types of camera tube. The slitless spectroscope will use a Type B uvicon without the barium-fluoride window.

Figure 7 shows how the detector will be placed within the optical system. After being reflected from the secondary mirror, light passes through the optical filter and is imaged onto the photocathode of the television tube. Since the electronic configuration of the tube requires that the photocathode have a radius of curvature of 3.15 inches concave toward the inside of the tube, the faceplate on which the photocathode is deposited takes the form of a very strong double-concave lens. The outer radius of curvature is 1.669 inches, allowing us to use a primary optical system having no curvature of field.

As figure 9 shows, these tubes have an extreme outside diameter of 2.75 inches. The photocathode covers an area 1.4 inches in diameter on the inside of the faceplate. The scanned area is 1.0-inch square. The resolution of the best tubes approaches 250 line pairs.

We expect to use exposure times between 0.1 and 100 seconds. Since these tubes can only integrate the signal from an ultraviolet image when high voltage (-15,000 volts) is applied to their photocathodes, we have no need for a mechanical shutter. We merely turn the high voltage on and off to regulate exposure time.

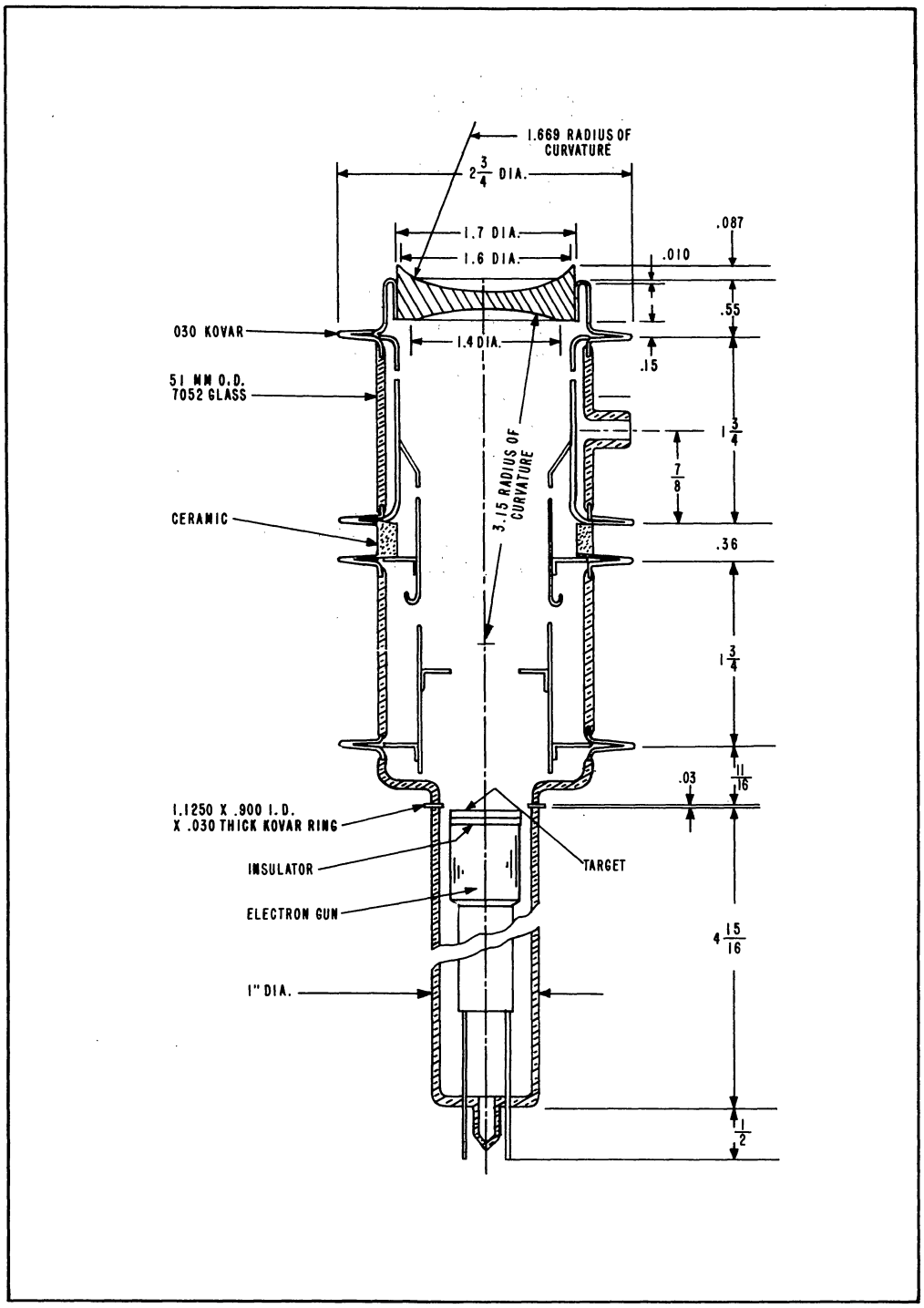

Figures 9A through 9C.--Prototype ultraviolet-sensitive ebicon. 9A.--Diagram.

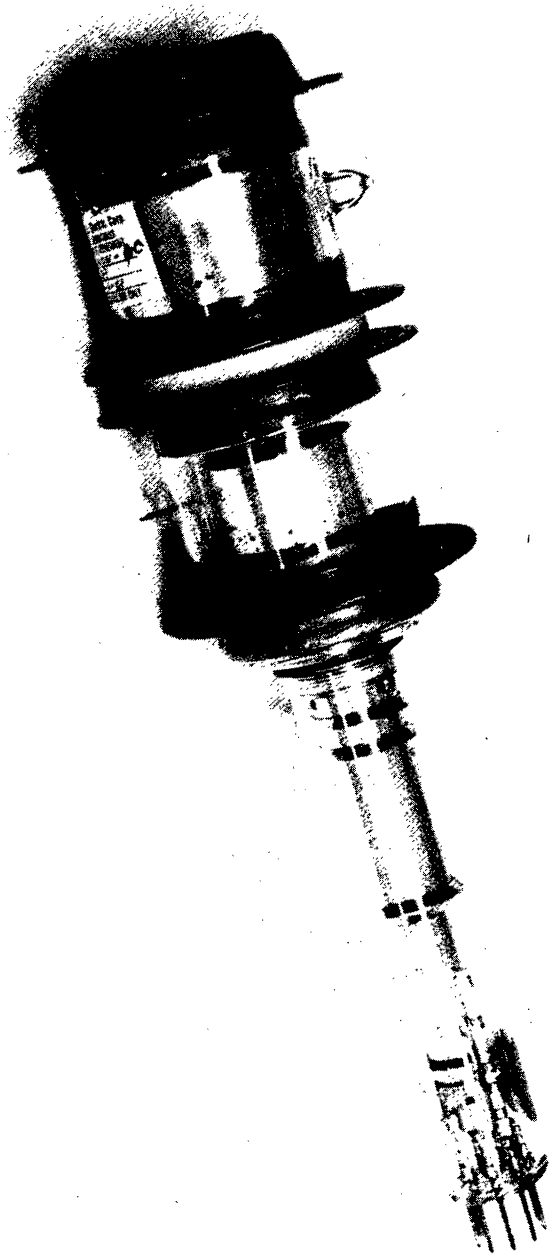

9B. --Photograph of ebicon.

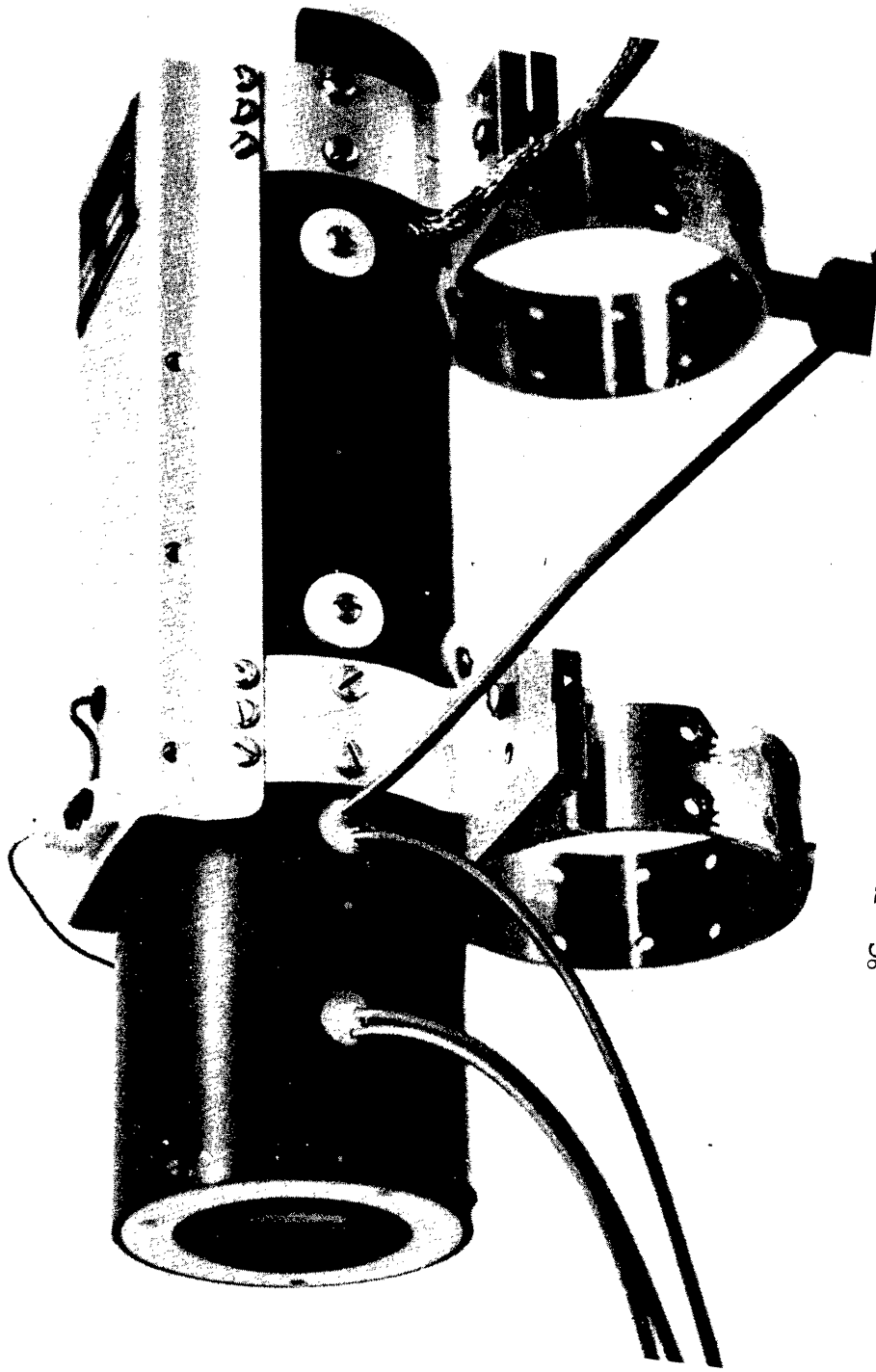

9C.--Photograph of ebicon in its mount.

For good focus, the electron-imaging section requires voltage ratios stable to 0.1 percent. The over-all accelerating voltage, however, can vary between 10 and 20 kilovolts without disturbing the focus. The nominal imaging voltages are -15.0 kilovolts, -14.4 kilovolts, -14.1 kilovolts, and ground. The ebic target is nominally at +50 volts.

The present ebic target consists of a freely supported aluminum-oxide film about 0.1 micron thick, mounted on a stainless-steel ring. On this substrate is evaporated a conducting backplate of aluminum about 0.07 micron thick. The ebic material for most tubes manufactured to date has been arsenic trisulphide between 1 and 2 microns thick smoked onto the central area of the aluminum.

Arsenic trisulphide is not entirely satisfactory for this purpose. It must be kept between 0° and +50° C for proper operation; for optimum operation, the limits are +10° and +30° C. It is destroyed by temperatures exceeding +150° C. Tubes now being built use an arsenic disulphide target. The maximum storage temperature of this material is 110° C. The new targets are of more uniformly high quality than the old, and have shorter persistence. We also plan to experiment with zinc sulphide.

Both types of ebic target have exhibited excessively long persistence. Many scans are required to erase the image, and the image returns after a waiting period. The former type of storage, which is caused by retention of charge, can be overcome at the expense of repetitive scanning. The latter type of storage, which is more damaging, is caused by trapped carriers in the target material. More research into other target materials is required better to approach the ideal situation of completely destructive readout. The target must, however, be capable of storing the image for an indefinite period before readout. Fortunately, most of the known ebic materials have this property.

The electron-gun section is identical to that of an electrostatic vidicon. We have chosen electrostatic rather than electromagnetic focussing and deflection to enable us to reduce power and weight requirements, eliminate magnetic fields, and use simpler electronics in our digital scanning mode. Heater power is reduced to about one watt.

A major problem in the construction of this tube is proper ruggedization. The program will succeed only if the tubes are capable of surviving launch and of operating in orbit for one year.

Figure 10 indicates how the tube will be mounted with its high-voltage power supply and video preamplifier in the detector case. We will maintain the target at the proper operating temperature by conducting heat to it from the vicinity of the cathode heater. By proper choice of conducting and insulating sleeves, we can achieve any target temperature between the equilibrium temperature of the experiment container (about -30° C) and a temperature of several hundred degrees Centigrade approaching that of the heater itself. In its standby condition, the heater will consume about 80 percent of its full operating power; there will therefore be a minimal fluctuation in target temperature.

2. Optical System

The linear resolution and field of view of the Celescope are prescribed by the detector. In turn, these set limits of between 16 and 40 inches on the first basic parameter of the optical system, the effective focal length. For a 40-inch focal length, the field of view becomes 1°.5 square, and we require 25,000 pictures to cover the sky. We do not expect to have time during the useful

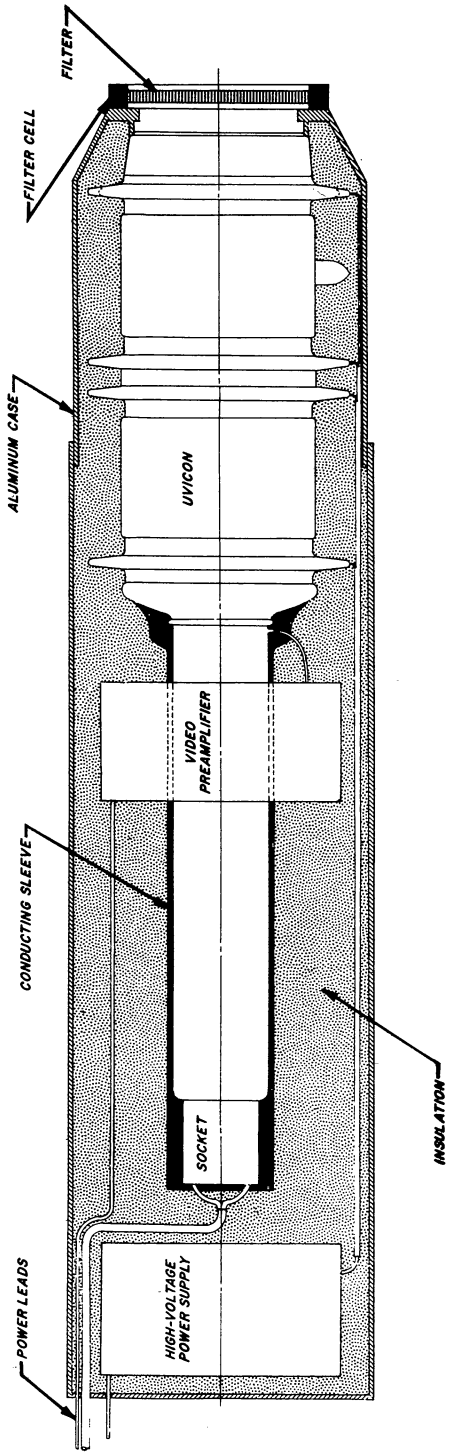

Figure 10.--Ebicon tube in detector case with high-voltage power supply and preamplifier.

life of this satellite to take more pictures than this. And it becomes very difficult to design a system of adequate aperture with a focal length as short as 16 inches. In addition, the resolving power decreases to 1 minute of arc and the densest fields would be expected to contain as many as 700 stars. Under such crowded conditions, we begin losing important information.

The second basic parameter of the optical system, the aperture, is set by the physical dimensions of the spacecraft that NASA is supplying. This aperture is 12 inches for each of our four instruments.

Within this framework, we require the simplest system that will give adequately small aberrations throughout our field of view. Complex instruments cannot adequately survive the launch environment. We cannot allow large lenses in our system, since they are not available in materials that are useful in the far ultraviolet. We studied the properties of one-mirror systems, and found none that could meet our requirements. In two-mirror systems, the Schwarzschild camera is the simplest that can fit our needs.

Schwarzschild (1905) designed this family of telescope to be free of coma, spherical aberration, and curvature of field. As applied to Celescope, this system gives nearly uniform, approximately circular star images about 50 microns in diameter, throughout a field of view 1.4 inches in diameter. Figure 7 shows the configuration.

We use a Schwarzschild camera with an effective focal length of 24 inches. The faceplate of the detector modifies the EFL to 24.893 inches. We have designed the system for no vignetting except in the corners of the field, since the shadow of the secondary mirror and its cell on the primary is larger than the perforation in the primary even for stars at the edges of the field of view 1-inch square. The reflection of this shadow by the primary mirror is over its entire length larger than the case containing the television camera tube. It is also larger than the perforation in the secondary mirror. Both mirrors are perforated for structural reasons associated with the launch environment and the detector case configuration. In addition, the light path for the calibration system passes through the perforation in the secondary.

The system has the following parameters:

Primary Mirror:

over-all diameter, 12.5 in.

clear aperture, 12 in.

perforation diameter, 5 in.

edge thickness, 2.2 in.

shape, hyperbolidal,

$$z = h^2/72\left(1 + \sqrt{1 + 0.000700h^2}\right),$$

where z is the sag and h is the height above the optic axis,

both expressed in inches.

reflecting surface, aluminum plus magnesium fluoride or lithium fluoride (Berning et al., 1960; Angel et al., 1961).

material, fused quartz

weight, 28 pounds

Secondary Mirror:

over-all diameter, 6.25 in.

clear aperture, 6.05 in.

perforation diameter, 1 in.

outside diameter of cell, 6.7 in.

edge thickness, 1 in.

shape, oblate ellipsoidal,

$$z = h^2/57.6(1 + \sqrt{1 - 0.012043h^2}),$$

where z is the sag and h is the height above the optic axis, both expressed in inches.

material, fused quartz

reflecting surface, aluminum plus magnesium fluoride or lithium fluoride

weight, 3 pounds

System:

effective focal length, 24.893 in.

total length between mirror vertices, 21.6 in.

distance between secondary mirror vertex and focal plane, 9.6 in.

field of view, 1 in. square = 2°.4 square

effective focal ratio ("transmission ratio"), T/3.7, assuming 75% reflectivity

sensory system: see above

image quality, 95% of light within 100-micron circle under all conditions of decentration less than .01 in. from optimum focus, throughout the field of view, for collimated input beam.

focal surface, plane except as modified by detector faceplate. See above.

weight, 44 pounds, including optics, detector, and telescope structure, but omitting integrating structure.

Although Schwarzschild's work was published in 1905, no Schwarzschild camera has ever been used successfully in astronomical research. Two such instruments, one at Brown University and one at Indiana University, proved ineffective because of the difficulty of figuring the optics, and because of the inconvenient location of the focal plane. For ground-based astronomy, the Schmidt camera gives much better performance. In space, however, the Schwarzschild system is far preferable. First, the Schmidt corrector plate poses great difficulties for work in the ultraviolet because of the small choice and sizes of transmission optical materials that are available. Second, the field of view and the resolution of our television system are too poor to enable us to take advantage of the superior resolving power and field of view provided by a Schmidt system. And third to withstand the rugged environment of launch, it is easier to mount small thick mirrors than large, thin corrector plates. It is true that Schmidt systems have been designed with reflective corrector plates, but such systems must be built off-axis with consequent difficulties in figuring and mounting them.

All four optical systems will be mechanically identical. The fourth will be a slitless spectroscope, with an objective grating ruled directly onto the surface of the primary mirror of a Schwarzschild camera. The requirement is that a stellar spectrum be spread out over about half the field of view, the region of spectral sensitivity being about 1100 to 2200 A. The ruling required to achieve this dispersion is 200 lines per millimeter. In order to suppress the unwanted orders and to accentuate what is expected to be the fainter end of the spectra of most stars, this grating should be blazed for Lyman-alpha ($0.^{\circ}25$ blaze angle). Since resolution is limited by the detector, we do not require a resolving power of the grating greater than 10 percent of the theoretical one. Our requirements cannot be met by ruling the grating onto the secondary mirror, since the best resolving power such optics would give us is 100 A, corresponding to 1.25 millimeters if the spectrum is 0.5 inch long.

Several of our requirements are severe, and we are not yet assured that such a grating can be produced. The blank diameter of 12.5 inch is larger than the 8-inch maximum usually handled. We are reluctant to settle for the decreased light-gathering power that would result were we to rule only the incribed square 8.5 inches on a side, but ruling of the entire 12-inch aperture poses especially difficult problems. The central perforation is another difficulty, probably not so serious. The rather steep curvature of the blank poses a third problem, especially in regard to blaze angle.

The ultraviolet calibrator already mentioned is also shown in figure 7. A small lamp, probably mercury vapor in a quartz envelope for all but the shortest wavelength (Type C detector), provides illumination for an artificial star field consisting of a pattern of pinholes 50 microns in

diameter. This pattern is focussed directly onto the photosensitive surface of the television camera tube by means of a lithium-fluoride lens. The optical path, folded by a plane mirror, passes through the central perforation of the secondary mirror. By varying the duration of the flash, this system can generate artificial stars having between 3×10^4 and 3×10^6 photons per image within the detector pass band. Intensity discrimination of the electronic system will be checked, since the pinholes will be calibrated and will differ slightly in size.

3. Mechanical System

The Celescope mechanical system can be considered in two sections: telescope modules and integrating structure.

The purpose of the structure for the telescope modules is to hold the various elements of the optical system in correct alignment. One of the primary considerations in our design of the Schwarzschild system was the allowable decentration error. Decentration is the departure, in any dimension, of an optical element from its position for optimum focus. Our system as designed will allow a decentration of any component parallel to the optic axis, up to 0.010 inch. Perpendicular to the optic axis, it will allow decentration of the primary mirror by 0.050 inch, of the secondary mirror by 0.025 inch, and of the faceplate of the television camera tube by 0.015 inch. No component may be tilted by more than 3 minutes of arc. Within these limits, image size throughout the field of view is less than the detector's resolution limit of 100 microns.

The temperature at which the Celescope must operate is $-30^\circ \pm 15^\circ$ C. The laboratory in which it must be adjusted prior to launch will, however, have a temperature of $+20^\circ \pm 10^\circ$ C. Since we require that the Celescope have no moving parts, we must choose structural materials that will preserve the proper dimensional relationships between the optical components over a temperature range of up to 75° C.

We have two alternatives for solving the problem of thermal expansion. The first is to build our optical components and structure from materials with the same coefficient of expansion. Unless this coefficient is negligible, this method requires that all structural elements be at the same temperature. In addition, mechanical considerations point toward a choice of structural materials with a medium or high coefficient of expansion, whereas optical considerations point toward optical materials of negligible coefficient of expansion.

Although we are investigating the use of novel techniques for obtaining dimensional stability from such low-expansion materials as Pyroceram, our primary effort is now directed toward the second method, that of passive compensation. The usual method of compensation makes use of two concentric cylinders, the shorter of which has a higher coefficient of expansion. These two cylinders are joined at one end. The distance between the free ends then remains constant regardless of temperature.

We plan to make use of the optical properties of the Schwarzschild system to simplify our compensation network. As shown in figure 7, the main structural tube between the primary and secondary mirrors will be titanium, approximately 25 inches long between the back surfaces of the two mirrors. The thermal expansion coefficient of titanium is about 8.5 parts per million per degree Centigrade, so that a drop of 75° C between room temperature and operating temperature will cause the distance between the mirrors to decrease by 0.016 inch. Although this distance exceeds our decentration limit, we can achieve adequate focus by moving the detector faceplate 0.023 inch nearer the primary mirror. If the temperature of the television-tube support is the

same as that of the titanium structure joining the two mirrors, aluminum is the correct material for joining the television-tube faceplate to the base of this titanium structure. If the heat released by the television tube cannot be removed by conduction before reaching the tube support and heating it, the correct material is magnesium. Aluminum has a coefficient of expansion of about 21.4 parts per million per degree Centigrade; magnesium has a coefficient of 27.1 parts per million per degree Centigrade.

During launch, the Celescope will be pointed downward, a deciding factor in our mirror-cell design. Each primary mirror will be supported by three padded fingers both on the outer rim and around the perforation. The back of this mirror will be supported by four teflon pads, and there will be three similar pads about its circumference. The 280-pound (10g) effective launch weight will be supported by the three fingers on the front side.

The support system for the secondary mirror will be similar to that of the primary. Here, however, the 30-pound (10g) effective launch weight will be supported by the padded back-plate.

The integrating structure is illustrated in figure 11. Most of this structure is being provided as part of the spacecraft in Grumman's experiment "can." Figure 12 is a photograph of this "can." The main support structure is an X-beam approximately 18 inches deep and 2 inches wide separating the four telescope modules. This beam is attached to the spacecraft through four mounting lugs. It is surrounded by a cylindrical ring for added strength. At the back end, secondary beams are attached to the primary X-beam and the ring. The telescope modules are attached to these secondary beams. The dust cover is attached to the ring. Additional integrating structure may be required between the front end of the X-beam and the front ends of the telescope modules.

The Celescope will be so constructed that the individual optical elements and the individual modules can be properly aligned in the laboratory. Each individual instrument will be adjusted to within .001 inch of optimum focus. The optical axes of the three broad-band television photometers should be parallel to each other and to the zero-order optical axis of the slitless spectroscope within 5 minutes of arc. This alignment must be calibrated in the laboratory, and maintained in space, to within 15 seconds of arc.

4. Electronic System

Figure 13 illustrates the operation of the electronic system. This system takes maximum advantage of our knowledge of the information content we may expect in our ultraviolet pictures.

Let us first consider the stellar component. We expect the ultraviolet sky from the standpoint of information to be very much like the visible sky. Most of the information is contained in the point sources, or stars. Our nebular pictures will contain not nearly so much information, even though we use a much higher sensitivity to obtain them.

Two characteristics distinguish a stellar from a nebular signal in the camera-tube output. First, and most characteristic, the time derivative of the stellar signal is much greater than that of the nebular signal. Second, and most easily dealt with, the amplitude of the stellar signal is expected to be much greater than that of the nebular signal. In Celescope we will make use of this second characteristic, and will consider any signal below an adjustable threshold to be zero. We wish to study with great accuracy the amplitudes and positions of any signals above threshold.

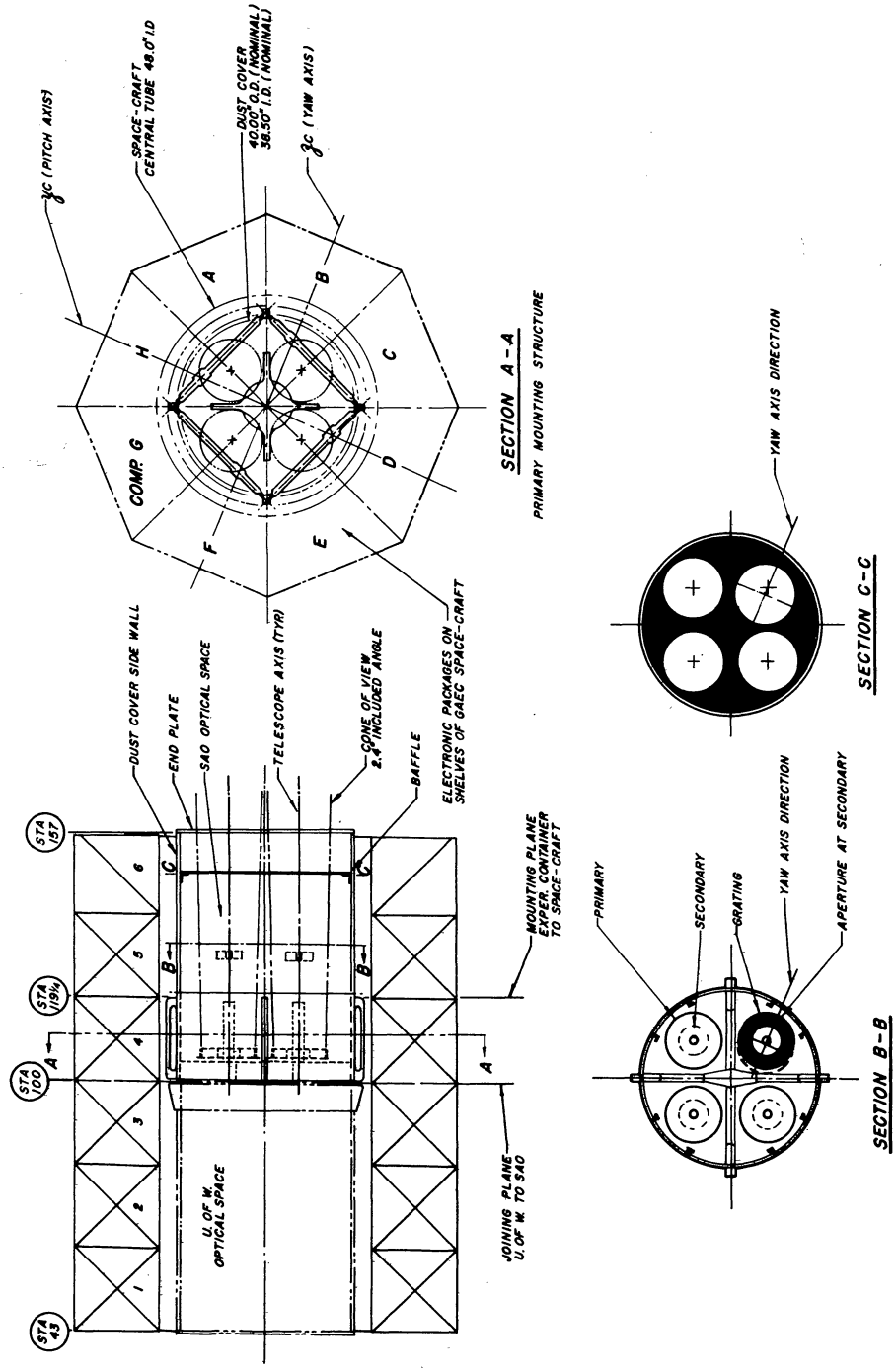

Figure 11.--Celescope in relation to the spacecraft.

Figure 12.--Photograph of spacecraft experiment container for Celescope.

1962SAOSR..83.....D

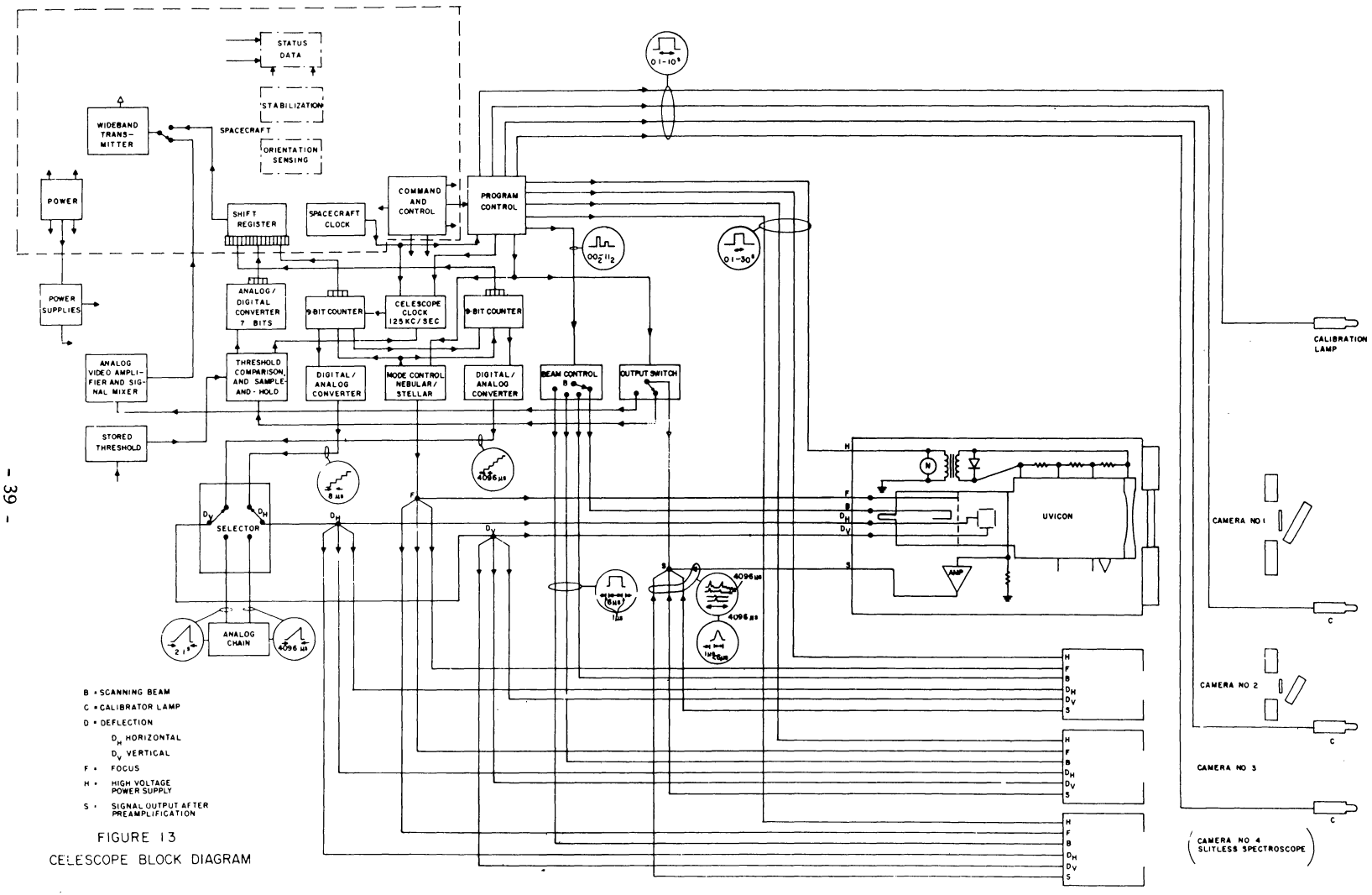

FIGURE 13
CELESCOPE BLOCK DIAGRAM

Figure 13.--Block diagram of Celescope electronic system.

If we were to transmit the entire picture in the usual way on a communication channel of constant power and bandwidth, we would be wasting most of the information potential of the system by transmitting zeros. Even the densest star fields, at our sensitivity are expected to fill only 0.4 percent of the area of the picture with useful information. Our communication system would then limit the accuracy of our received information. The obvious solution is to digitize.

The easiest way to accomplish positional digitization is to deflect the beam with a staircase sweep derived from a clock. If we take 2^9 steps across the face of the tube we are assured that the tube itself, rather than the deflection system, is limiting the resolution. We thus allow the Celescope clock to drive a 9-bit counter, which in turn drives a digital-to-analog converter to derive the horizontal staircase deflection voltage. This first counter also drives a second 9-bit counter from which we derive the vertical staircase voltage. The clock-pulse separation, set to give a basic scan time of 2 seconds, is 8 microseconds.

In order to eliminate the effect of transients in the staircase voltages, the scanning beam is on for 6 microseconds, delayed by 1 microsecond from the time of rise of the staircase deflection voltage. Thus, the scanning beam does not show transients and the quality of the picture is not affected. Since the presence of the scanning beam is necessary for obtaining an output signal, the beam-control unit can serve a second purpose and act as the camera-selection switch.

For stellar operation the output switch connects the camera outputs to the analog-to-digital converter. The output of this converter is compared in the threshold unit with the threshold-set register; any signal greater than the setting on the register stops the clock and causes the output of the analog-to-digital converter to be combined with the settings of each of the 9-bit counters and to be sent to the spacecraft's shift register as a 25-bit parallel binary word. This word is transmitted via the spacecraft's wide-band transmitter at a rate of 12.5 kilobits per second. After a 2.5-millisecond delay the clock is re-started and the process continued. With the maximum count of 250 stars, we expect 1000 picture elements to exceed threshold. Under these conditions, our scan time will be 4.5 seconds per camera. With the average count of 14 stars, the total scan time will be slightly more than 2.1 seconds per camera.

A nebular scan is achieved by the same type of staircase sweep. In order to increase the sensitivity for the anticipated weak signals, the beam is de-focussed and one to three bits of each counter are shorted out. The current density of the beam is maintained constant by increasing total beam current. The output from the cameras is now sent to the wide-band transmitter in the usual analog television fashion, through an analog video amplifier with 62-kilocycle-per-second bandwidth. The analog sweep chain will be used only if the digital chain fails.

The exposure control (or electronic "shutter") is the application of high voltage to the imaging section of the camera tube. Through the spacecraft's command system we can control the length of each individual exposure by adjusting exposure times initially to give a convenient anticipated amount of data, and changing them thereafter only to compensate for changes in system sensitivity.

In our electronics laboratory we have built a breadboard version of the digital television system. This model has demonstrated the feasibility of such a method. The input is an electrostatically-scanned vidicon that can observe a photograph of a star field. Later, the vidicon will be attached to a telescope for actually viewing the sky. It is scanned by the digital mode of figure 13 to produce the output described on p. 69 (below) and in figure 20C. Figure 14 shows this breadboard equipment.

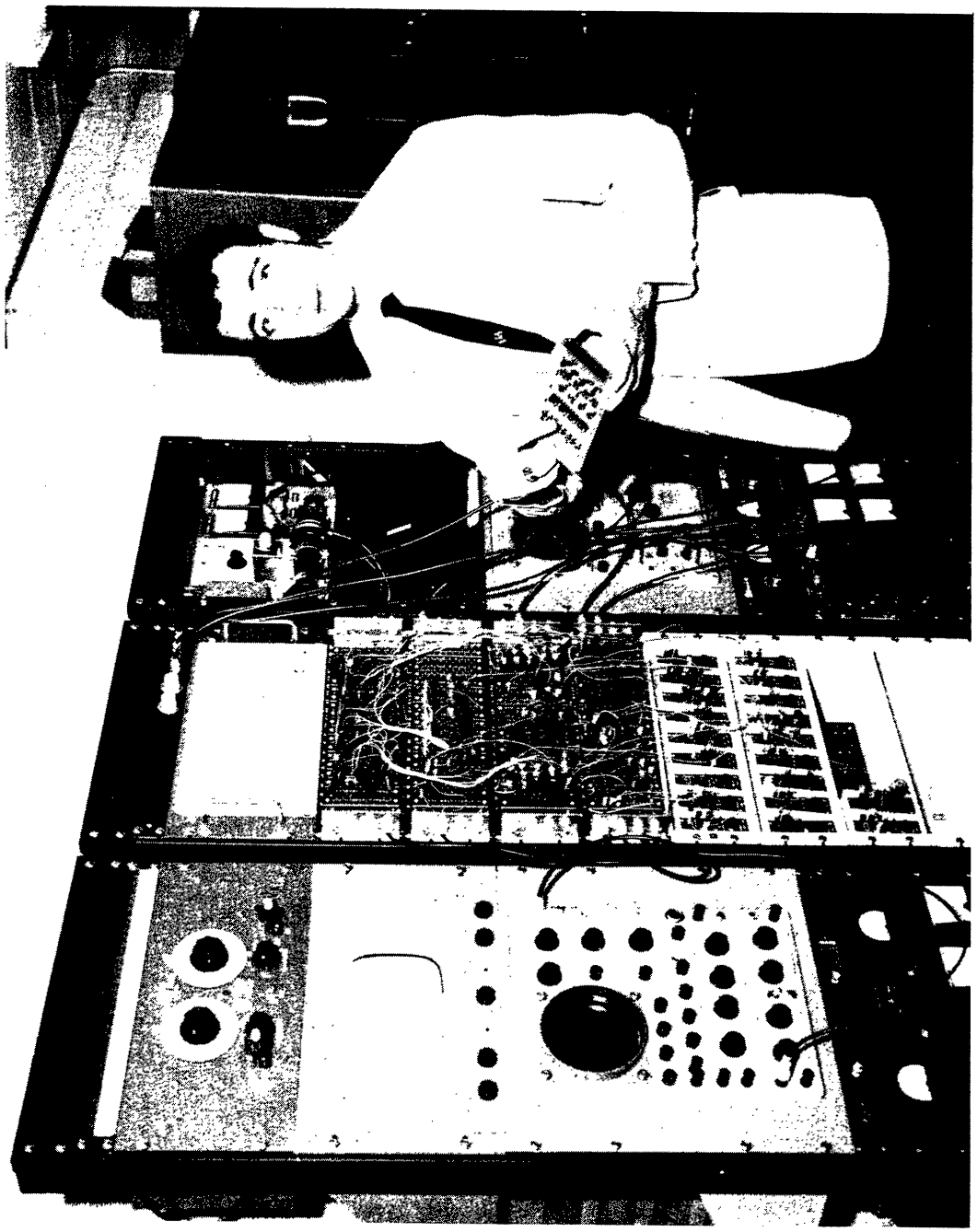

Figure 14. --Breadboard digital television system. Mr. Arazi holds one of the building blocks used in the construction of the model.

Figure 15A indicates one possible sequence of operations for a single slew direction. In general, only two commands need be transmitted to the spacecraft to initiate the entire sequence of operations for an active pass over the ground station.

The first command, carried out five minutes before the expected beginning of radio contact, is to slew the spacecraft to its initial position. At the same time the Celescope electronic equipment is energized, and polarization is commenced for all four camera tubes. Polarization is accomplished by flooding the ebic target with electrons from the reading gun, most probably scanning an enlarged beam at rather high beam current. The purpose of polarization is to bring the entire target to the potential of the cathode, thereby erasing any image that may be stored there. In ordinary television, polarization and readout are accomplished in the same repetitive scanning operation.

The second command, initiated by actual radio contact with the spacecraft, is to commence the sequence illustrated in figure 15A. Polarization is terminated by a signal from the spacecraft indicating that the satellite has stabilized in the position commanded. An interlock in the Celescope prevents the initiation of the operational sequence until one second after the end of polarization.

The Celescope-clock time for execution of each of the 21 individual camera commands is set into a register in Celescope, and can be changed when necessary through the command and control systems. The other important Celescope operating parameters may also be set in a similar manner. These include the Celescope-clock time for initiating the three slews scheduled during each pass, the times for turning on and off the calibrator lamps, the number of vertical and horizontal lines in the scanning raster for both nebular and stellar scan, the control voltages of the uvicons, etc.

Figure 15B illustrates a typical sequence of operations to be made during an active pass. At the center of the initial slew, when the stars are trailing at their maximum rate, the calibrator lamps and high voltage supplies are turned on for a calibration as free as possible from stellar interference. Again after the last slew the system is calibrated by means of the lamps, but with a stationary star pattern. Since this entire sequence can be completed in five minues, we would have time during each active pass of the satellite to conduct two additional slewing operations if enough power were available.

5. Reliability

Probably the most severe requirement that we have placed on the Celescope is that of reliability. Even with rather optimistic assumptions about the efficiency of our mapping operation, we will need about eight months to complete the survey. To give us a reasonable chance of fulfilling our objective, we have specified that the Celescope have a 70-percent probability of operating for one year in orbit. NASA has specified the same reliability figure for the space craft.

This level of reliability implies a mean time to failure for the entire Celescope of more than two years, since the system will be operated for several hundred hours during test and countdown. We consider the system to have failed when the mean operating efficiency of the Celescope has fallen to 10 percent. We define the operating efficiency as the product of the Position, Intensity, and Threshold performance criteria indicated in figure 16. The stellar and nebular operating efficiencies of the four cameras are combined to give us our mean.

A: Initiate stellar exposure.
B: Terminate stellar exposure.
C: Initiate stellar scan.
D: Initiate slitless spectroscope exposure.
E: Initiate nebular exposure.
F: Terminate nebular exposure.
G: Initiate nebular scan.
H: Terminate slitless spectroscope exposure.
I: Terminate slew.
J: Initiate slew.

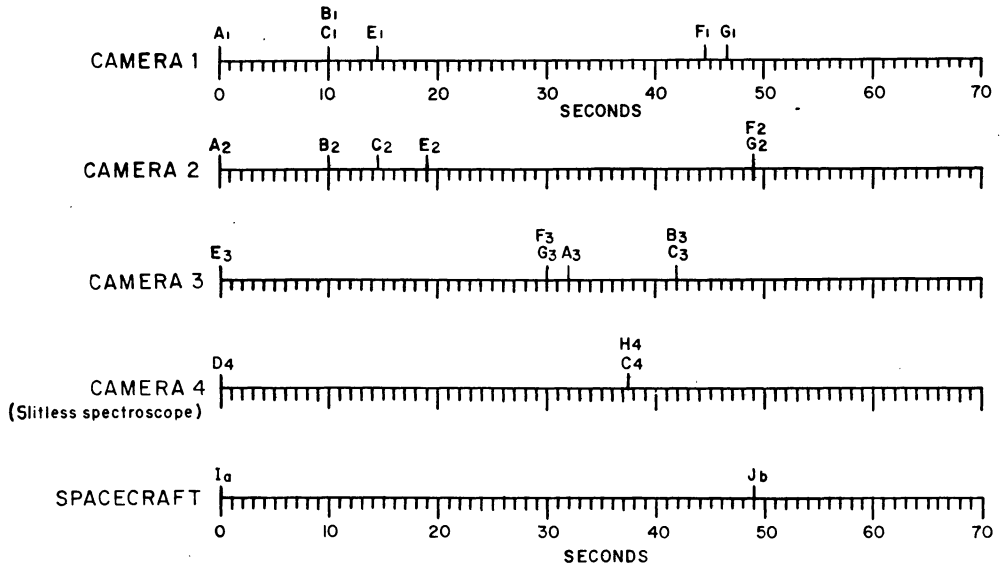

Figure 15.--Sequence of operations for Celescope in orbit. 15A.--Operations at one slew position.

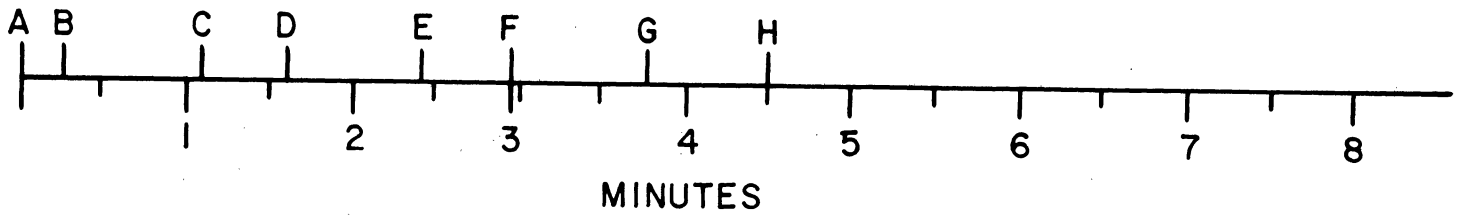

A: Commence scanning the calibration exposures.

B: Commence operations in first position.

C: Commence second slew. Read out status data.

D: Commence operations in second position.

E: Commence third slew. Read out status data.

F: Commence operations in third position.

G: Commence second calibration.

H: End second calibration.

15B.--Operations during one active pass over a ground station.

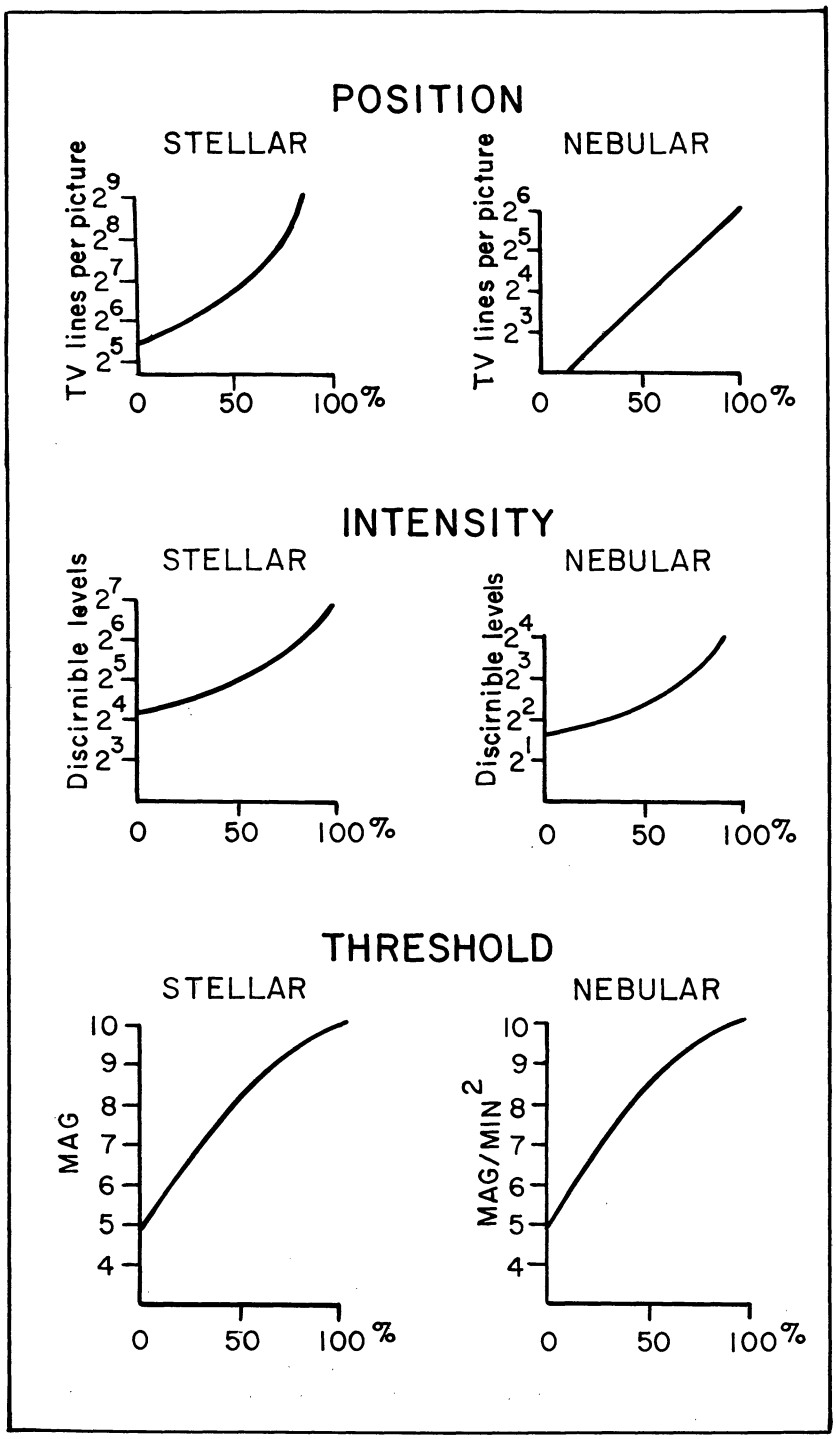

Figure 16.--Celescope performance-level criteria.

It appears that the most critical elements of the Celescope are the television camera tubes. These are the only electronic components in the system for which no reliability figures are yet available, and for which we cannot use redundant circuit design to circumvent failures. Our experience with prototype tubes indicates that we may expect the mean time before failure of a uvicon tube to be at least six months.

By applying the same design and production techniques used on such satellites as Tiros and Explorer, we should be able to achieve mean time to failure for the remainder of the Celescope system in excess of the required two years. These techniques, of course, take into account the rugged environments of shipping, test, launch, and space. We must therefore take into account the effects of high and low temperatures, humidity, vibration, shock, acceleration, weightlessness, extremely high vacuum, electromagnetic and corpuscular radiation, and magnetic field. Ferromagnetic materials cannot be used in appreciable quantities because of the effect on satellite stability of their interaction with the earth's magnetic field. Materials of vapor pressure higher than 10^{-10} mm of mercury cannot be used because they would evaporate too rapidly in the vacuum of space.

IV. Requirements on Spacecraft

1. Optical System

The aperture stop of the optical system -- 12 inches -- is at the primary mirror, near station 100 at the center of the spacecraft. To keep the system free from vignetting, the clear aperture must increase by 6 inches for each 100 inches of distance from the stop. At the secondary, the aperture must be 13.5 inches, and at station 158.25 -- the end of the optical "can" -- it must be 15.5 inches. The aperture at the radiation shield, 40 inches from the primary mirror, must be 14.5 inches. Except for the slitless spectroscope, these openings must be centered over each primary mirror. Figure 11 indicates the positions and sizes of these openings.

The nominal resolving power of the detector, operating at 256 line-pairs per inch, is about 30" of arc. Each of the other sources of blurring -- optical aberrations, decentration of the optical components, and image motion -- should individually be kept to 15" of arc or less. Since the maximum anticipated exposure is one minute, our requirement for spacecraft stability is 15" of arc for one minute of time. Since Celescope will not generate an error signal, this degree of stability must be maintained by the coarse control system of the spacecraft. (See below).

2. Mechanical System

Figure 11 indicates the mechanical interface between the Celescope and the spacecraft. Each of the four telescopes is attached to three tie-points to the base plate. The base plate -- part of the optical "can" furnished by Grumman -- is attached to an X-frame 18.5 inches deep and 2 inches wide. This frame, the main structural member of the optical "can," is tied to the spacecraft structure through four tie-points at station 120.

Each of the three broadband photometers will weigh about 44 pounds, with the center of mass at about station 115 on the optic axis. The slitless spectroscope will be identical structurally to the other three cameras.

The radiation shield is 40 inches above the primary mirrors, near station 145. It shields the detectors from direct illumination from the sky, helps maintain the heat balance of the container, and helps to shield against damaging radiation. It can be a very thin aluminum sheet, preferably attached directly to the dust cover. No other structure, however, should be attached to the cover.

Each detector case will liberate about 0.8 watt of heat in the standby condition, 1.0 watt in the on-condition, and 3.5 watts during exposure.

Electronic equipment other than that contained in the detector case will be mounted in Bay E4 of the spacecraft (fig. 11). This equipment will probably be contained in 5 boxes, each 10.5 x 6.5 x 3 inches and weighing 8.9 lbs. Cables and connectors will weigh about 5.0 lbs. The heat dissipation will be about 1.5 watts per box.

3. Control Requirements

As mentioned above, the coarse control system of the spacecraft must be able to maintain stability of the optic axis of 15" of arc for one minute of time.

The basic Celescope experiment has no absolute a priori requirement for accurate knowledge of the position of the optic axis. We do require that adjacent positions be separated by $2^{\circ}.2 \pm 0^{\circ}.1$ about one of the two major axes perpendicular to the optic axis. The experiment can become nearly 90 percent efficient if we know the starting position to within 1°, and approaches 50 percent of somewhat lower efficiency if our control of the starting position is in error by more than 10°.

In most parts of the sky, a map $2^{\circ}.2 \times 6^{\circ}.6$ should be sufficient to determine unambiguously the direction, but the reduction would be extremely difficult. The finder television to be installed as part of the spacecraft will make this a posteriori positional reduction much faster and easier, should the positional control system aboard the spacecraft fail.

The Celescope will not provide an error signal to the spacecraft's fine control system. Should the control system fail, but we still have manual ground control over the inertia wheels and inertia dumping mechanism, we could complete our mapping by stabilizing the television picture at the beginning of each pass and slewing a controlled number of coarse-wheel turns between positions.

4. Power Requirements

The following power requirements are maxima allowed by our specifications. Figure 17 is based on these maxima, although the actual power consumption will probably be somewhat smaller. Power reduction below these levels can be converted to additional slewing capacity at the rate of approximately 4° of slew per watt per orbit.

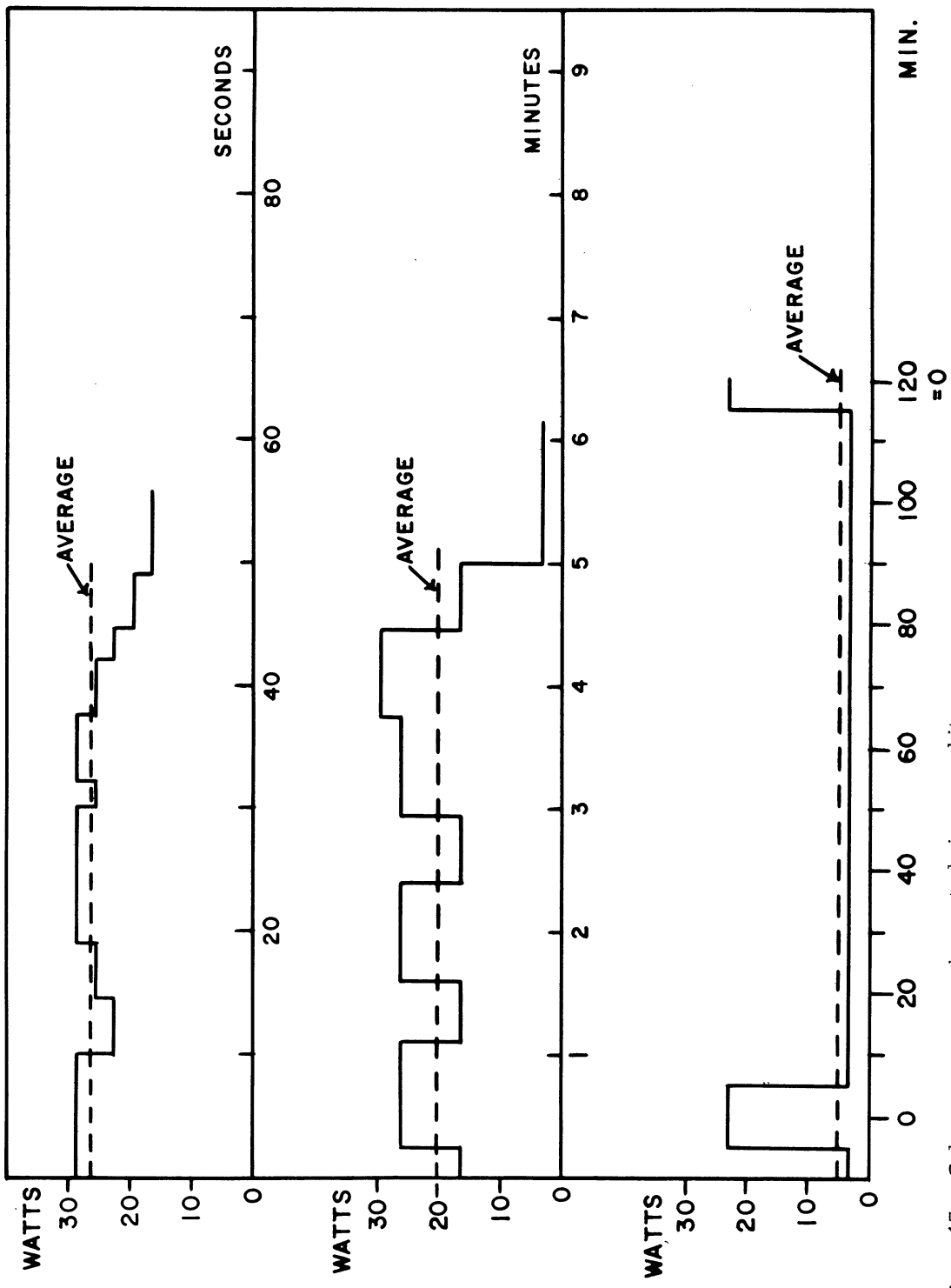

Figure 17.--Celescope power requirements during one orbit.

High-voltage power supplies:	3.0 watts apiece
Video preamplifiers:	0.1 watt apiece
Camera-tube heaters:	1.0 watts apiece operating 0.8 watt apiece standby
Calibrator lamps and power supply:	10 watts
Remaining electronics:	12 watts

Figure 17 reflects the operating sequences illustrated in figure 15.

The power is to be supplied from the spacecraft as $+28.0 \pm 0.1$ volts D.C., 1.05 amperes maximum current. The over-all average power consumption is 4.8 watts.

5. Slewing Requirements

The basic limitation on the rate at which the Celescope can map the sky is the slewing capability of the spacecraft. As noted above, we are limited to a basic limit of three slews per orbit, of $2\overset{\circ}{.}2$ each.

6. Data-Handling Capability

Our contemplated short exposure should provide photometric data on 100,000 stars in each of three broad spectral regions. The long exposures will give information concerning nebulosities, and provide spectroscopic data on about 5,000 of the brighter stars.

In the initial phases of the program, we will adjust the exposure time for each of the broad-band television photometers to bring the extrapolated total number of stars observed by that instrument to the desired level of 100,000. The transfer characteristics of the detector, together with the stellar intensity-distribution function and the duplication of stars resulting from our planned 10 percent overlap in adjacent fields of view, will cause these stars to be registered by our system as 1,900,000 binary words of 25 bits each. Each of our four stellar television instruments will generate one-fourth of this amount during the mapping operation. This data will be contained in pictures taken in at least 8520 directions.

If we divide our number of binary words by the number of slews required to complete them, we obtain an average of 225 words per slew. Because of the non-random distribution of stars, the maximum number is expected to be about 18 times this value -- 4050 words, or 100,000 bits, per slew; or 25,000 bits per slew per photometer. The spacecraft bit-transmission rate of 12,500 bits per second would thus allow us to transmit our maximum expected data in 2 seconds per camera. As can be seen from figure 15A, we are allowing 4.5 seconds for these scans in our preliminary thinking, including 2 seconds during which the Celescope is examining "black" areas and not transmitting information. We easily have time available if necessary to double this quantity.

In addition to our digital data, we will have analog data occupying 6 or 8 seconds per slew, at 62 kc/sec bandwidth.

Figure 15B indicates that we plan to take 4 minutes to complete our three slewing operations. The exact schedule of operations can be adjusted to the needs of the program. We will be using the wide-band transmitter about half the time during each pass, including transmission of calibration and status information.

7. Data Storage and Readout Capability

We do not now plan to utilize the data storage available in the spacecraft. There is ample time available during the "expose" period at the start of our first scan to unload the information stored in this memory from the University of Wisconsin experiment.

We do plan to use the spacecraft shift register associated with this memory to match our 25-bit parallel Celescope digital output with the spacecraft transmitter.

8. Experiment Commands

Under normal conditions, the entire sequence of operations will be stored in a set of registers in the Celescope electronic system. This sequence will be initiated by the combination of a signal from the spacecraft that it has stabilized at the first slew position, and a signal from the command receiver that the spacecraft is in communication with a ground station. The signal to slew to this first position will come from a command stored during the previous pass. The command will include information equivalent to the galactic longitude and latitude of the optic axis, and the time of initiation of slewing. This slew will be timed for completion 5 minutes prior to the estimated time of establishing contact with the ground station.

We now expect to have available to Celescope, 13 command lines, with 12 bits per command. These lines will be used primarily to re-set the Celescope registers. The registers will control the following functions:

For each of the four individual cameras:

For data runs:	Bits	Channels
1. Detector high-voltage focus controls	4	3
2. Detector beam-focus control, nebular	4	1
3. Detector beam-focus control, stellar	4	1
4. Detector-beam-current control, neb.	4	1
5. Detector beam-current control, stel.	4	1
6. Detector target-voltage control, neb.	4	1

	Bits	Channels
7. Detector target-voltage control, stel.	4	1
8. Number of lines in scan, nebular	4	1
9. Digital-scan intensity threshold	4	1
10. Time to initiate stellar exposure	9	1
11. Time to terminate stellar exposure	9	1
12. Time to initiate stellar scan	9	1
13. Time to initiate nebular exposure	9	1
14. Time to terminate nebular exposure	9	1
15. Time to initiate nebular scan	9	1
For calibration:		
16. Time to initiate exposure	9	1
17. Time to end exposure	9	1
18. Time to commence scan	9	1
For over-all program control:		
1. Time to commence nth calibration	9	8
2. Time to commence nth slew of $2^{\circ}.2$	9	8
3. Time to commence reading out status data nth time	9	8
4. Axis about which nth slew is to be performed	1	8

These requirements can be supplied with only 11 of the 13 available lines, since by appropriate use of the first few bits each line can be split into several channels of less than 12 bits.

9. Experimenter's Status Data

As indicated in figure 18, the experimenter's status data are to be read out and transmitted once for each slew position. These status data must include the reading of each of the registers indicated above, in addition to about 50 key voltage-levels throughout the Celescope electronic equipment, and temperatures at about 10 locations. They must also include spacecraft status data, such as gimbal angles, sufficient to determine the pointing direction.

$\begin{matrix} DC \\ 1 \end{matrix}$ = Digital scan, calibration exposure, camera #1.

$\begin{matrix} D1 \\ 2 \end{matrix}$ = Digital scan, first slew, camera #2.

DS = Digital transmission, status data.

$\begin{matrix} A \\ 1 \\ 3 \end{matrix}$ = Analog scan, first slew, camera #3.

etc.

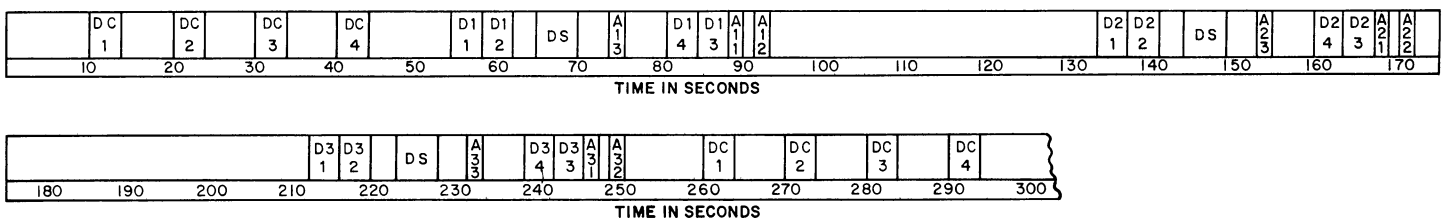

Figure 18.--Sample format for Celescope data tape.

V. Ground-Support Equipment

The Celescope ground support equipment has three functions: to test and calibrate the Celescope during production, testing, and count-down; to perform a prompt and accurate reduction of the data; and to assist in necessary adjustment of the Celescope in orbit as necessary.

Figure 18 indicates the format of data on the raw data-tape that would result from the sequence of operations shown in figure 15. This tape is recorded on the FR-600 tape recorder at NASA's ground station. It will contain short bursts of analog information interspersed with longer groups of digital information each having a word length of 25 bits. A second tape-channel will contain timing information from the master clock at the NASA ground station. Although Celescope's portion of the signal channel will correspond closely to the output format given by the Celescope to the spacecraft, the blank spaces of figure 18 may actually contain data either from the University of Wisconsin equipment or from the spacecraft.

Fortunately, the NASA ground station contains a General Mills computer and an IBM digital tape recorder that includes an IBM-729 tape transport. This equipment will be able to translate the information on the raw data-tape into a format suitable for input to an IBM-7090 computer. The Celescope ground-support equipment will therefore not need to incorporate this translation circuitry into its digital signal-conditioning unit.

Under normal conditions, the General Mills computer and the IBM-729 tape transport will be used to convert the output from the raw data-tape into more useful form. The computer will be programmed to recognize the various types of information contained on the FR-600 tape.

Our analog pictures, of 62 kc/sec bandwidth, will be converted to digital form by pulse-code modulation. In this type of modulation, the computer must sample the amplitude of the waveform at a rate of 124 kilosamples per second, numerically equal to twice the highest frequency of the video signal. Since we require at least 20 shades of gray, these samples must be digitized to 5-bit accuracy. The PCM data-rate must be 620 kilobits per second to accommodate 5 bits at a rate of 124 kilosamples per second. The General Mills computer together with the FR-600 has this data-rate capability for PCM conversion. However, we must either store temporarily each picture while the IBM-729 digital tape recorder reads out the information at the slower rate of 300 kilobits per second, or we must reduce to one-half the playback speed of the FR-600 at the input to the chain.

Our digital pictures and status information will be converted and recorded in correct format for later input to an IBM-7090 computer. Irrelevant information will be omitted from the converted tape. The General Mills computer will assign a serial number to each picture as it is converted into correct IBM format.

The Celescope ground-support equipment will consist of portable equipment and a fixed installation. Figure 19A is a block diagram of the portable equipment, which can be transported by two men and a station wagon. It will be used as necessary to analyze the performance of the Celescope during manufacture, testing, pre-launch count-down, and orbital operations. It will also allow an accurate check of the correctness of the format conversion performed by NASA's General Mills computer. Figure 19B is a block diagram of the fixed installation, to be used in Cambridge for final data analysis and for preparation of the observational results for publication.

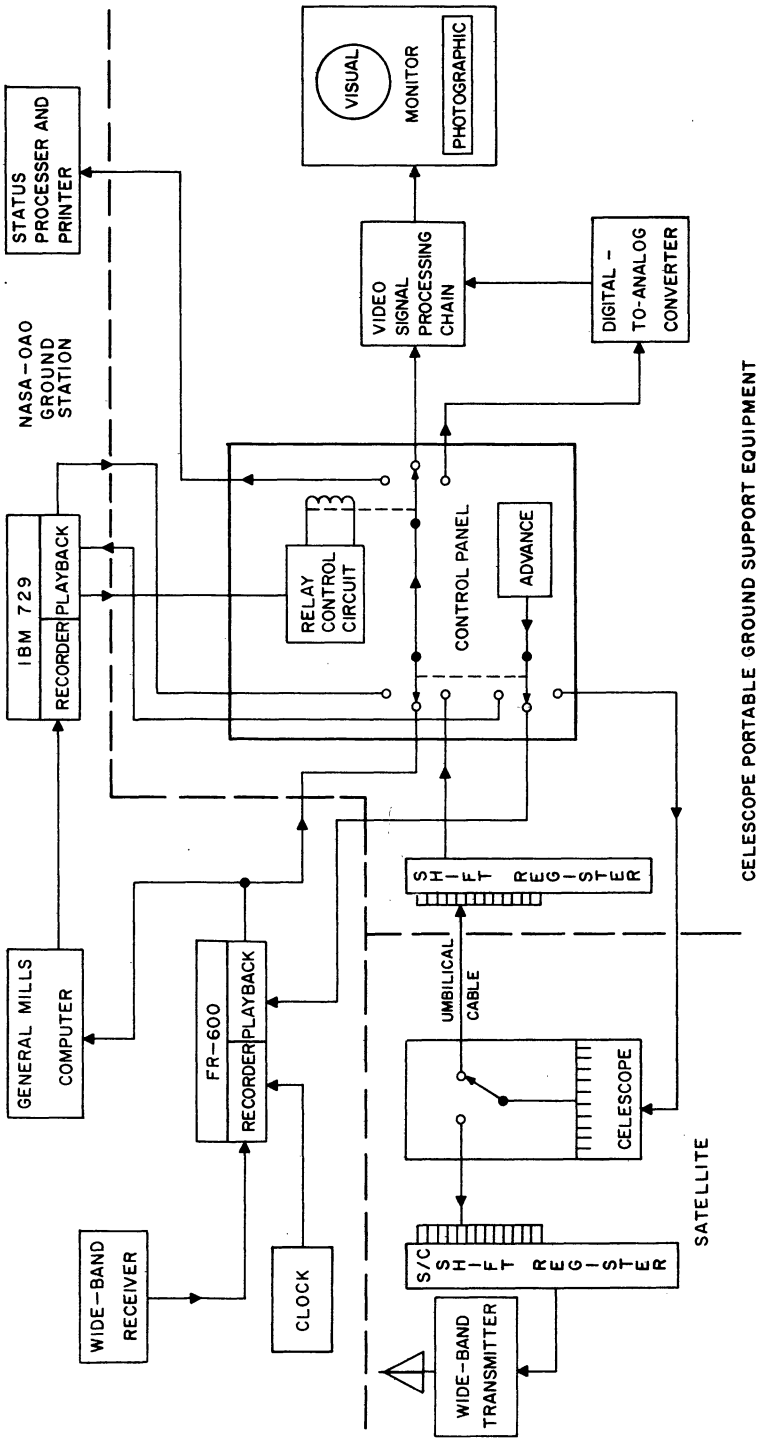

Figure 19.--Simplified block diagram of Celescope ground support equipment. 19A.--Portable installation.

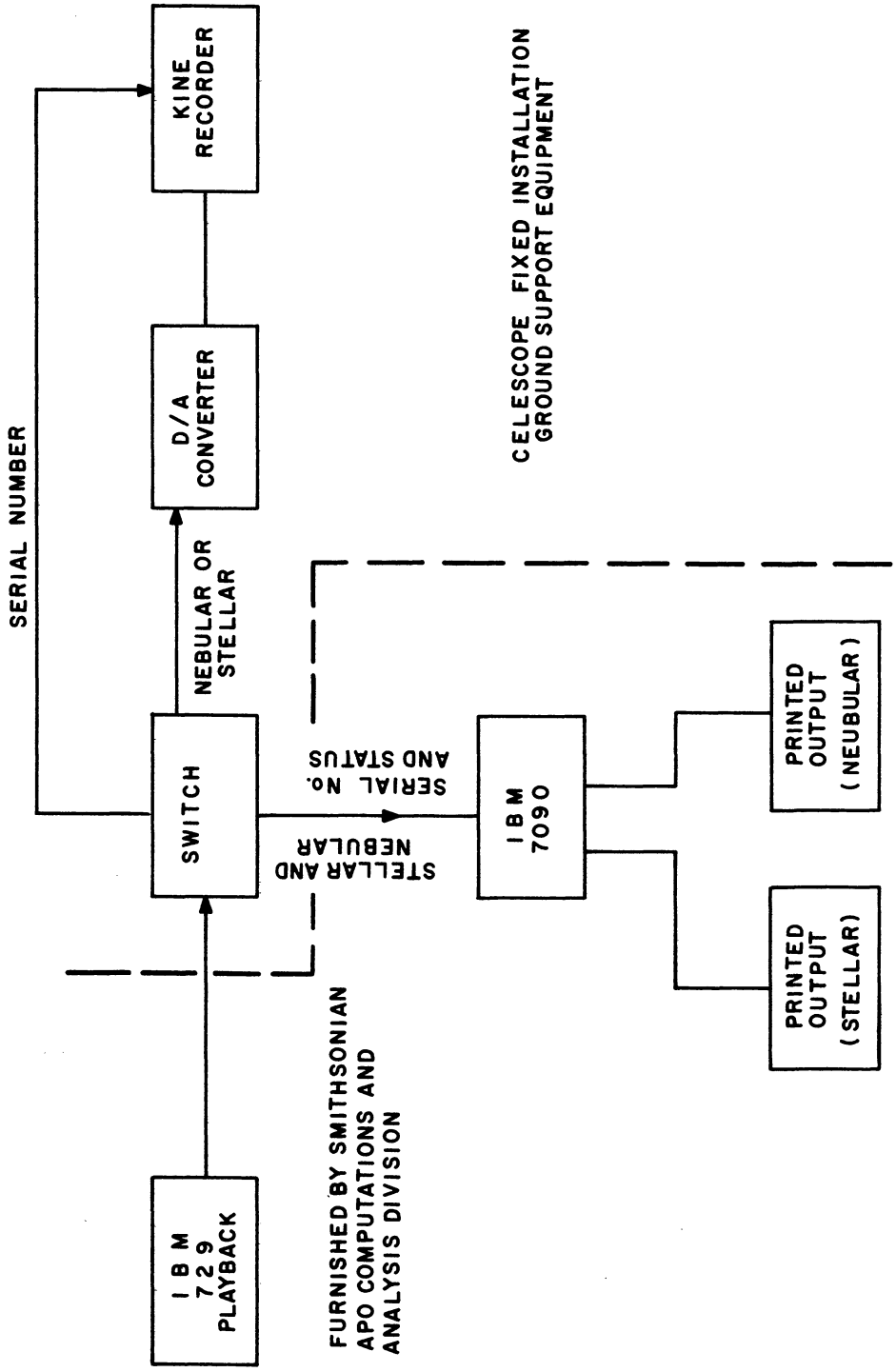

19B.--Fixed installation.

The main control unit for the portable installation is nothing more than a switching panel. Prior to launch, it is set to accept a signal directly from the Celescope. This input line may also be connected to the video output from NASA's wide-band receiver or from the FR-600 recorder, since these signals have closely related formats. With such direct data input, the output must be set manually to either the digital or analog mode. Pushing the "advance" button on the control console will then cause the Celescope to generate and transmit one frame from the sequence, or will cause the FR-600 tape recorder to advance one frame.

For normal post-launch operation, the control unit of the portable installation will be set for automatic control by the FR-600 tape, as well as by the IBM-729 tape. The operator will choose each time which tape he desires as input. In this mode, the signal from the tape sets the output switches automatically. Pushing the "advance" button again allows the tape to advance by one frame.

From the control panel, the digital signals are routed to the digital-to-analog converter, which converts both the Celescope stellar pictures and the PCM nebular pictures to proper analog form for display. Analog nebular pictures from the raw data-tape, as well as the output from the digital-to-analog converter, are sent to the video processing chain, and thence to the monitor, where they are stored for prolonged viewing until the next push of the "advance" button. The operator may view the picture on the long-persistence viewing screen of the monitor, or he may use a Polaroid camera to record the picture on the other screen for more detailed study. For study of a complete series of pictures, he may use an automatic 35-mm camera to record the series without interruption.

Status data are sent from the control unit to the status processor and printer present in NASA's ground station. These data may be presented to the Celescope operator in any visible form that is convenient, since their sole use will be for comparison with the current set of experiment instructions. To facilitate the comparison, these current instructions will be made available in a format identical to this display. The data format conversion performed by the General Mills computer will include an automatic comparison between status data and instructions. All status information contained in the IBM-729 tape will thus either be verified or flagged for special investigation and treatment.

Figure 19B is a block diagram of the fixed installation, in Cambridge, of the ground-support equipment. The converted data tape will be played back from the IBM-729 tape transport for direct input to an IBM-7090 computer. The computer will utilize the status data, the digital stellar picture data, the PCM nebular picture data, and the serial number information to prepare catalogs of the brightnesses and spectrophotometric curves of ultraviolet stars, isophotal contour maps of the PCM pictures, and a table describing the picture associated with each serial number.

With the IBM-729 tape transport connected to the Celescope ground-support equipment rather than to the IBM-7090 computer, the nebular and stellar pictures are sent to a digital-to-analog converter and thence to a slow-scan high-resolution "kinerecorder" where a full gray-scale photograph is taken of each picture. The serial number is automatically illuminated in the margin. The operator may choose to expose both the stellar and the nebular picture of a given region of the sky together on the same frame by overriding the double exposure prevention in the kinerecorder. The photographs can then be published along with the catalogs.

VI. Data Reduction

Our astrophysical analysis would be accomplished by running the digital record as the data input to a digital computer program for the generation of our star catalog, and by measuring the isophotal contours and kinescope records for investigating the nebulosities and for a quick idea of the stellar data. We feel that we must be able to use simultaneously the scientific judgment for a subjective data analysis, and the automatic computing methods for an objective data analysis. Our main provision for the former is to make no decisions that will prevent useful data available in the satellite from reaching the ground. Our main provision for the latter is our digitization of stellar brightness and position information on board the satellite. The digital information will be more accurate and easier to handle than the analog information. We plan to organize a digital computer program for processing these data into a printed star catalog. The magnetic-tape equivalent of this printed catalog can then easily be used for further studies of stellar atmospheres, and for use in computing programs that, because of our present inadequate knowledge of stellar ultraviolet fluxes, cannot be specified in advance.

In addition to the star catalog, we will produce ultraviolet maps of the sky, showing both stars and nebulosities, and an atlas of stellar spectrophotometric curves in the ultraviolet. Since the dispersion of the slitless spectroscope will be perpendicular to the horizontal scan direction, spectral information will behave the same way in our digital communications link as will stellar photometric information. The computer will recognize spectra from their position in the picture sequence and will handle them accordingly.

We believe that these catalogues will provide a wealth of data on which to base theoretical papers. We will therefore publish them without undue delay, to allow study by other members of the astronomical community.

In our laboratory we have prepared a breadboard model of both the space-borne and ground-based data handling equipment shown in figure 14. We are utilizing two types of display for evaluation of these data-handling techniques, as illustrated in figure 20.

The multiple A-scope presentation of figures 20A and 20B enables us to measure the brightnesses of nebulae and stars as a function of position, throughout the entire field of view, by standard astronomical measuring engines. This multiple A-scope monitor has independent controls for its intensity and its amplitude modulation. Under the low magnification shown in figure 20A we can examine the intensity-modulated picture directly to see what it looks like. Under the high magnification shown in figure 20B we can measure the amplitude and waveform of the signal precisely. In the operational version of the ground support equipment, these functions will be accomplished by the PCM encoding, followed by analysis with the 7090 computer.

In the operational version of the ground-support equipment, the digital presentation of figure 20C will also not normally be presented in visible form, but rather will be fed directly to a computer. Each column of dots represents a picture element for which the intensity was above threshold. The first 18 bits give the position of the picture element, and the last 7 bits give its intensity.

Tables 1 and 2 are prototype samples of the catalogs we plan. Figure 21 shows samples of the pictures that will be published and studied along with these catalogs. Note that figure 20 consists of photographs of a breadboard display system used to evaluate the data processing equipment philosophy. Figure 21 is our conception of how the actual display will look.

Figures 20A through 20C.--Sample pictures from breadboard data-analysis monitors (photographs). 20A.--Multiple A-scope display.

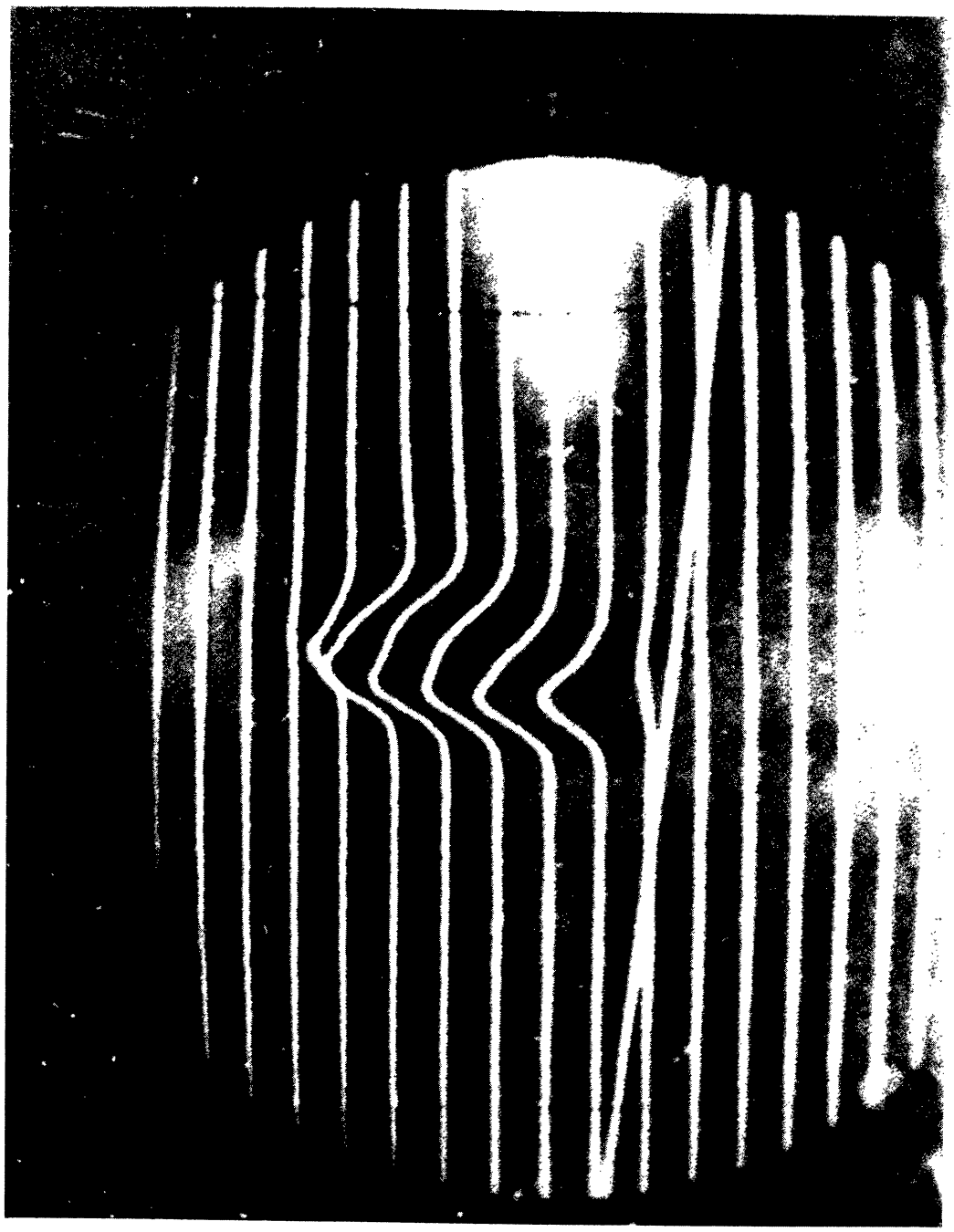

20B.--Enlargement of 20A.

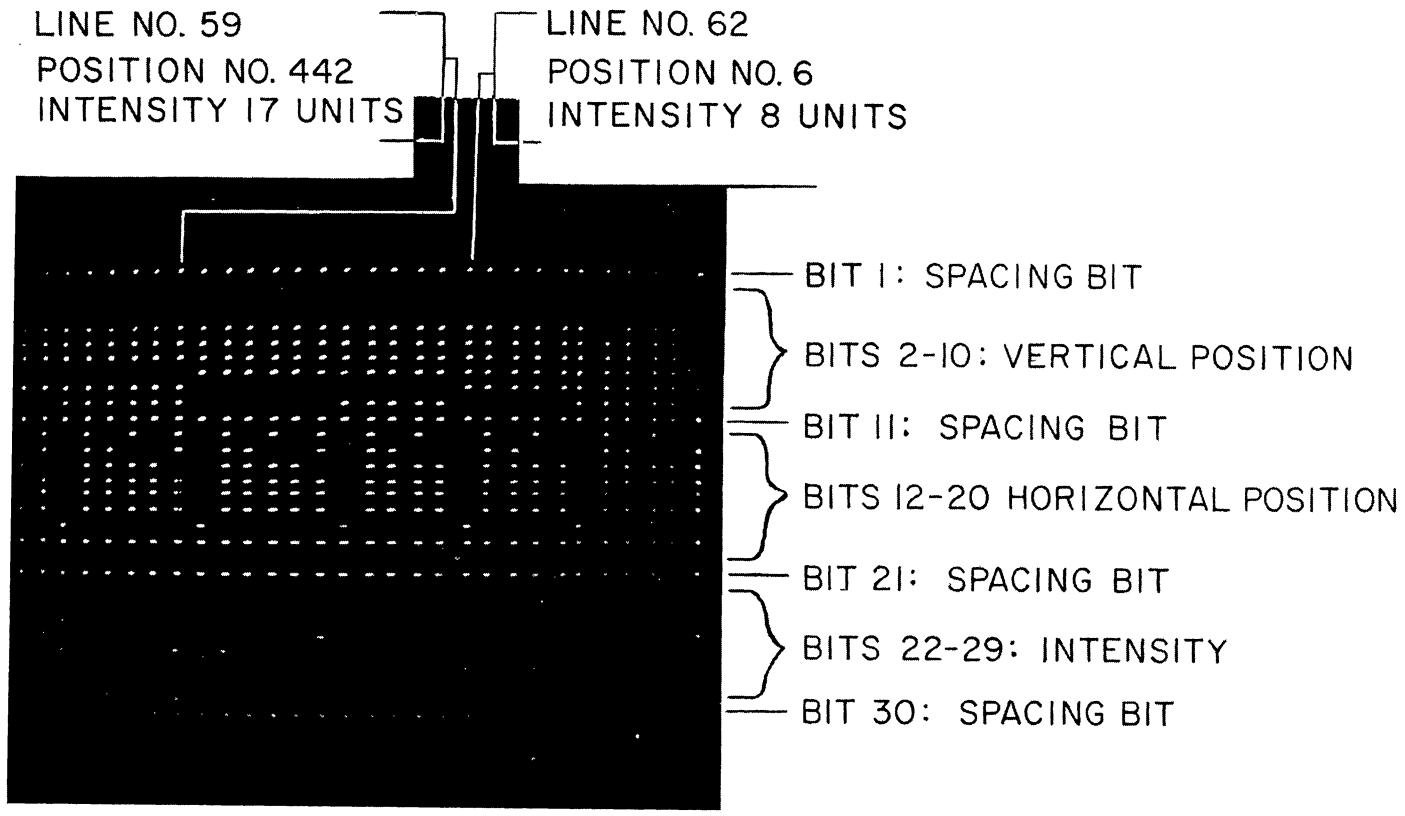

20C.--Digital display.

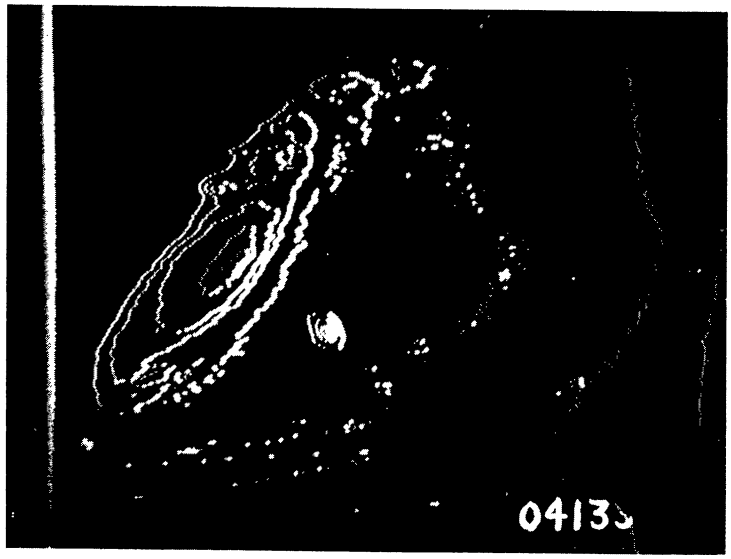

Figures 21A through 21C. --Sample pictures from operational data analysis monitors (artist's conception). 21A. --Isophotal contours.

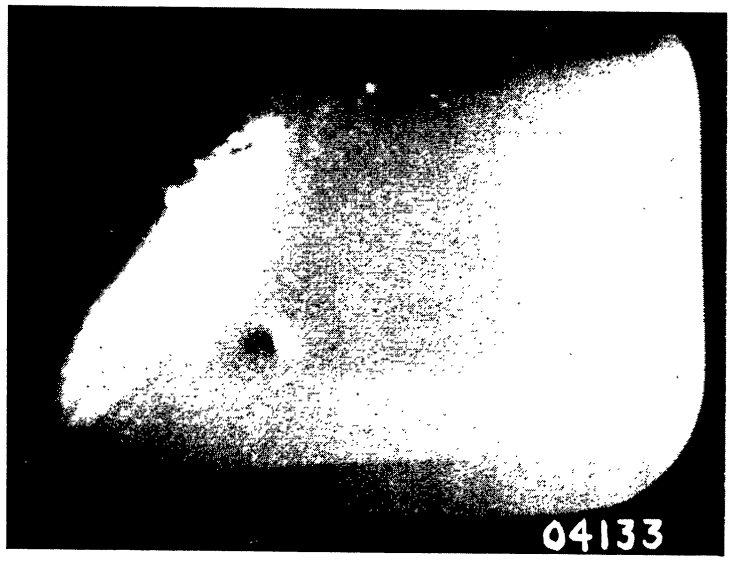

21B. --Ultraviolet map.

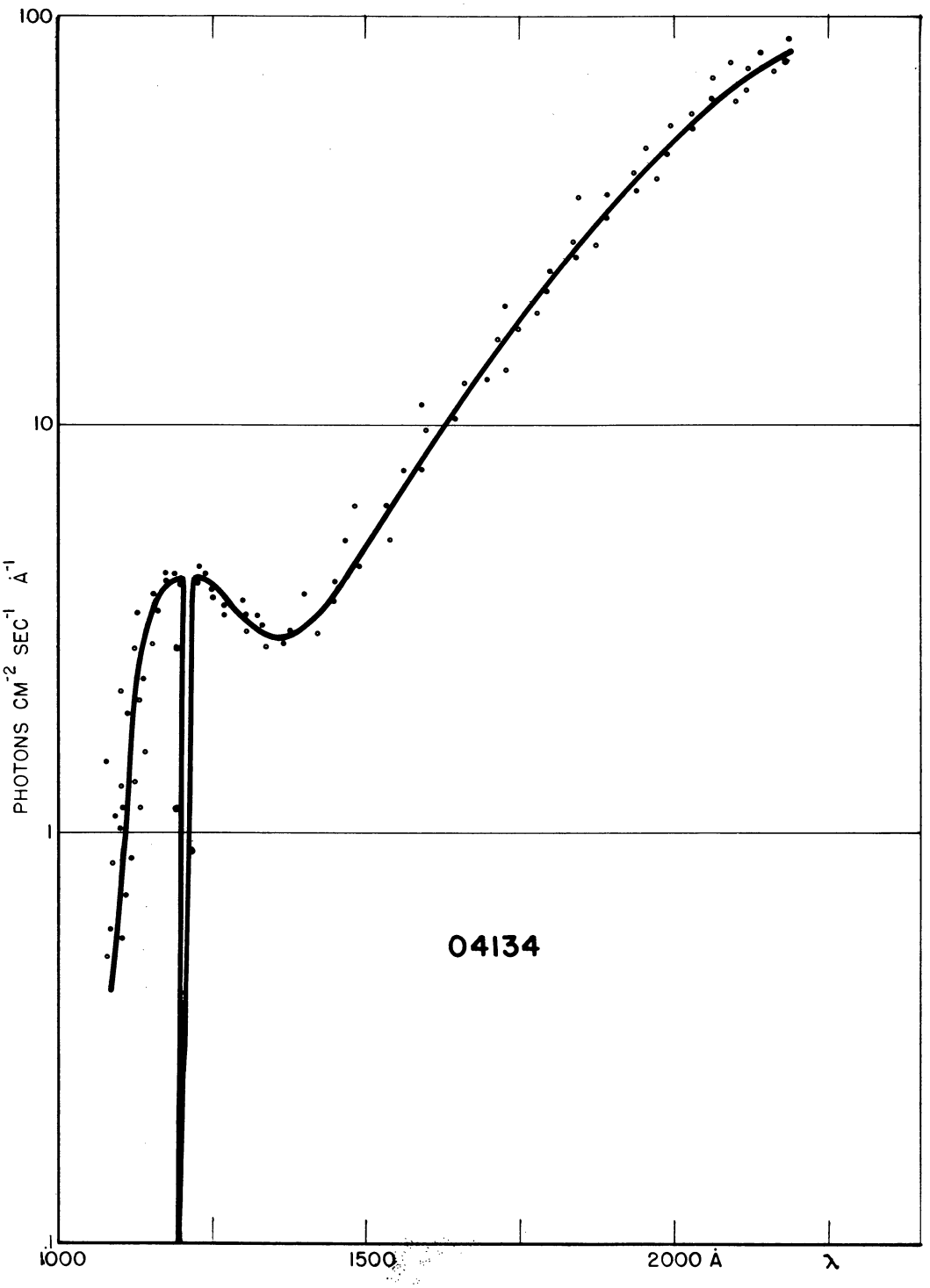

21C. --Spectrophotometric curve from slitless spectroscope.

Table 1--Sample catalog of ultraviolet stellar magnitudes

Celescope Catalog Number	(1950.0) Right Ascension	Declination	m_{u1} (2200 A)	m_{u2} (1600 A)	m_{u3} (1350 A)	m_{u4} (S. S. 0-order)	Spectrum	m_{pv} (5300 A)
18100	$5^h\ 33.^m5$	+07.°93	8.7	9.3	---	9.3	---	---
18101	5 33. 6	-13.06	---	---	9.5	---	---	---
18102	5 33. 7	-01.23	0.3	-1.0	-2.3	-2.0	cB0eI	1.8
18103	5 33. 9	+15.57	9.5	---	---	---	---	---
18104	5 33. 9	-53.49	---	9.5	9.5	---	---	---
18105	5 34. 0	+00.27	7.9	7.5	7.8	---	---	---
18106	5 34. 2	+61.55	8.9	9.6	---	9.9	---	---
18107	5 34. 3	+21.12	1.9	0.9	-0.1	-0.3	B3pe	3.1
18108	5 34. 3	-06.09	4.8	3.1	1.8	2.5	B1	5.8
18109	5 34. 5	-03.32	---	9.8	7.5	8.1	---	---

Table 2--Sample table describing published pictures

Serial Number	Center coordinates (1950.0) Right Ascension	Declination	Exposure Time	Camera Number	Resolution (TV Lines)	Zenith Distance	Scanning Mode	Threshold (Stellar Magnitude)	Exposure Start Time
									JD2438456 +
04130	$0^h\ 38.^m7$	$+28.^\circ17$	$10.^s0$	3	512	80°	S	10.0	.93700
04131	0 38. 7	+30.37	5.7	1	512	79	S	9.5	.93778
04132	0 38. 7	+30.37	8.3	2	512	79	S	9.8	.93778
04133	0 38. 7	+30.37	30.0	3	128	79	N	----	.93778
04134	0 38. 7	+30.37	30.0	4	512	79	S	9.6	.93778
04135	0 38. 7	+30.37	29.3	1	256	79	N	----	.93795
04136	0 38. 7	+30.37	25.8	2	128	80	N	----	.93801
04137	0 38. 7	+30.37	10.0	3	512	80	S	10.0	.93813
									JD2438457 +
04138	0 47. 5	+25.95	5.7	1	512	60	S	9.5	.00454
04139	0 47. 5	+25.95	8.3	2	512	60	S	9.8	.00454

References

In addition to the specific references in the text, the following general reviews may prove helpful:

BERKNER, L. V., and ODISHAW
1961. Science in space. McGraw-Hill Book Company, New York, 458 pp.

SCHATZMAN, E.
1960. Les applications de l'astronautique à l'astrophysique. Astronautica Acta, vol. 6, pp. 159-166.

SWINGS, P.
1961. Report of Commission 44, In Agenda and draft reports, 11th General Assembly, International Astronomical Union, Willmer Bros. and Hara Ltd., Birkenhead, England, pp. 521-555.

WHIPPLE, F. L., and DAVIS, R. J.
1960. Proposed stellar and interstellar survey. Astron. Journ., vol. 65, pp. 285-290.

Specific references

ALLEN, C. W.
1955. Astrophysical quantities. Athlone Press, London, 263 pp.

ANGEL, D. W., HUNTER, W. R., TOUSEY, R., and HASS, G.
1961. Extreme ultraviolet reflectance of LiF-coated aluminum mirrors. Journ. Opt. Soc. America, vol. 51, pp. 913-914.

BAEZ, A. V.
1960a. A self-supporting metal Fresnel zone-plate to focus extreme ultra-violet and soft X-rays. Nature, vol. 186, p. 958.

1960b. A proposed X-ray telescope for the 1- to 100-A region. Journ. Geophys. Res., vol. 65, pp. 3019-3020.

1961. Fresnel zone plate for optical image formation using extreme ultraviolet and soft X radiation. Journ. Opt. Soc. America, vol. 51, pp. 405-412.

BERNING, P. H., HASS, G., and MADDEN, R. P.
1960. Reflectance-increasing coatings for the vacuum ultraviolet and their applications. Journ. Opt. Soc. American, vol. 50, pp. 586-597.

BLAAUW, A.
1961. On the origin of the O- and B-type stars with high velocities (the "run-away" stars), and some related problems. Bull. Astron. Inst. Netherlands, vol. 15, pp. 265-290.

CARRIER, G. F., and AVRETT, E. H.
1961. A non-gray radiative-transfer problem. Astrophys. Journ., vol. 134, pp. 469-481.

DAVIS, R. J., and GODFREDSEN, E. A.
1961. Optimum resolving power for an ultraviolet space telescope. Journ. Planet. Space Sci., vol. 5, pp. 207-212.

GREENBERG, J. M.
1960. The sizes of interstellar grains. Astrophys. Journ., vol. 132, pp. 672-676.

HARTMANN, J.
1904. Investigations on the spectrum and orbit of δ Orionis. Astrophys. Journ., vol. 19, pp. 268-286.

HAYAKAWA, S.
1960. A possible origin of the ultraviolet radiation from galactic clouds. Publ. Astron. Soc. Japan, vol. 12, pp. 113-114.

HINTEREGGER, H. E.
1961. Telemetering monochromator measurements of extreme ultraviolet radiation. Part II: Physical applications. In Space astrophysics, W. Liller, ed., McGraw-Hill, New York, pp. 74-95.

HUNGER, K.
1955. Die Atmosphäre des AO-Sternes Alpha Lyrae. Zeitschr. f. Astrophys., vol. 36, pp. 42-97.

JOHNSON, F. S.
1961. Solar radiation. In Satellite environment handbook, F. S. Johnson, ed., Stanford University Press, Stanford, pp. 77-81.

KAMIYAMA, H.
1959. Vertical distribution of molecular oxygen. Sci. Rep. Tohoku Univ., ser. 5, vol. 11, pp. 84-97.

KUPPERIAN, J. E., Jr., BOGGESS, A., III, and MILLIGAN, J. E.
1958. Observational astrophysics from rockets. I. Nebular photometry at 1300 A. Astrophys. Journ., vol. 128, pp. 453-464.

MALITSON, H. H., PURCELL, J. D., TOUSEY, R., and MOORE, C. E.
1960. The solar spectrum from 2635 to 2085 A. Astrophys. Journ., vol. 132, pp. 746-766.

PIKEL'NER, S. B., SHKLOVSKII, I. S., and IVANOV-KHOLODNYI, G. S.
1959. On possible mechanisms of emission of discrete galactic objects in the spectral region 1225-1350 A. Astron. Journ. U.S.S.R., vol. 36, pp. 264-268.

SCHWARZSCHILD, K.
1905. Untersuchungen zur geometrischen Optik. II. Theorie der Spiegeltelescope. Mitt. Astron. Sternw. Göttingen, no. 10, 28 pp.

SCIENTIFIC AMERICAN
1960. Ultraviolet stars. Vol. 202, no. 3, pp. 88-89.

SHKLOVSKII, I. S.
1959. Corpuscular emission from early-type stars as a possible cause of emission from nebulae in the region 1225-1350 A. Astron. Journ. U.S.S.R., vol. 36, pp. 579-584.

SKORINKO, G., DOUGHTY, D. D., and FEIBELMAN, W. A.
1961. An ultraviolet sensitive image tube. Westinghouse Res. Lab., Scientific Paper 912-J902-P1, 6 pp; in press Journ. Opt. Soc. America.

STECHER, T. P., and MILLIGAN, J. E.
1961. Stellar spectrophotometry below 3000 Angstroms. Astron. Journ., vol. 66, p. 296.

STONE, P. H., and GAUSTAD, J. E.
1961. The application of a moment method to the solution of non-gray radiative-transfer problems. Astrophys. Journ., vol. 134, pp. 456-468.

STROM, S. E., and STROM, K. M.
1961. Interstellar absorption below 100 A. Publ. Astron. Soc. Pacific, vol. 73, pp. 43-45.

TOUSEY, R.
1961. Ultraviolet spectroscopy of the sun. In Space astrophysics, W. Liller, ed., McGraw-Hill, New York, pp. 1-16.

TRAVING, G.
1955. Die Atmosphäre des BO-Sternes τ Scorpii. Zeitschr. f. Astrophys., vol. 36, pp. 1-41.

UNDERHILL, A. B.
1951. A model atmosphere for an early O-type star. Publ. Dominion Astrophys. Obs. Victoria, vol. 8, pp. 357-384.

VIGROUX, E.
1960. L'ozone atmosphérique. L'Astronomie, vol. 74, pp. 241-255.

VITENSE, E.
1951. Der Aufbau der Stern atmosphären. IV. Kontinuierliche Absorption und Streuung als Funktion von Druck und Temperatur. Zeitschr. f. Astrophys., vol. 28, pp. 81-112.

WILSON, N. L., TOUSEY, R., PURCELL, J. D., JOHNSON, F. S., and MOORE, C. E.
1954. A revised analysis of the solar spectrum from 2990 to 2635 A. Astrophys. Journ., vol. 119, pp. 590-612.

ZIEMER, R. R.
1961. Orbiting astronomical observatories. Astronautics, vol. 6, no. 5, pp. 36 ff.